Economics and Human Biology 40 (2021) 100950

Contents lists available at ScienceDirect

Economics and Human Biology

journal homepage: www.elsevier.com/locate/ehb

Modelling children's anthropometric status using Bayesian distributional regression merging socio-economic and remote sensed data from South Asia and sub-Saharan Africa

Johannes Seiler[a], Kenneth Harttgen[b,*], Thomas Kneib[c], Stefan Lang[a]

[a] Department of Statistics, University of Innsbruck, Universitätsstr. 15, 6020 Innsbruck, Austria
[b] Department of Humanities, Social and Political Sciences, ETH Zurich, Clausiusstr. 37, 8092 Zurich, Switzerland
[c] University of Göttingen, Chair of Statistics, Humboldtallee 3, 37073 Göttingen, Germany

ARTICLE INFO

Article history:
Received 6 February 2020
Received in revised form 11 November 2020
Accepted 11 November 2020
Available online 2 December 2020

Keywords:
Anthropometric measures and growth failures
Childhood malnutrition Bayesian distributional regression
UNICEF framework of malnutrition
South Asia
Sub-Sahara Africa

ABSTRACT

A history of insufficient nutritional intake is reflected by low anthropometric measures and can lead to growth failures, limited mental development, poor health outcomes and a higher risk of dying. Children below five years are among those most vulnerable and, while improvements in the share of children affected by insufficient nutritional intake has been observed, both sub-Saharan Africa and South Asia have a disproportionately high share of growth failures and large disparities at national and sub-national levels. In this study, we use a Bayesian distributional regression approach to develop models for the standard anthropometric measures, stunting and wasting. This approach allows us to model both the mean and the standard deviation of the underlying response distribution. Accordingly, the whole distribution of the anthropometric measures can be evaluated. This is of particular importance, considering the fact that (severe) growth failures of children are defined having a z-score below −2 (−3), emphasising the need to extend the analysis beyond the conditional mean. In addition, we merge individual data taken from the Demographic and Health Surveys with remote sensed data for a large sample of 38 countries located in sub-Saharan Africa and South Asia for the period 1990–2016, in order to combine individual and household specific characteristics with geophysical and environmental characteristics, and to allow for a comparison over time. Our results show besides gender differences across space, and strong non-linear effects of included socio-economic characteristics, in particular for maternal education and the wealth of the household that, surprisingly, in the presence of socio-economic characteristics, remote sensed data does not contribute to variations in growth failures, and including a pure spatial effect excluding remote sensed data leads to even better results. Further, while all regions showed improvements towards the target of the Sustainable Development Goals (SDGs), our analysis identifies hotspots of growth failures at sub-national levels within India, Nigeria, Niger, and Madagascar, emphasising the need to accelerate progress to reach the target set by the SDGs.

1. Introduction

The risk of dying as a neonate or a young child is found to be higher for undernourished children, compared to those who are well nourished. A strong, positive relationship is found between the nutritional status and the risk of dying, and this holds particularly true for children with a low weight-for-height z-score (Pelletier et al., 1995; Pelletier and Frongillo, 2003; Bryce et al., 2005; Black et al., 2008, 2013; United Nations Children's Fund et al., 2017, 2019). While anthropometry does not reflect all aspects of nutrition (for example, anthropometric indicators do not account for micronutrient deficiencies), immediate and chronic nutritional deficiencies are well captured. Assessing growth failures using anthropometric measures is thus a useful technique to assess the health status of individual children as well as the general health status of a population at an aggregated level, for instance on a sub-national or national level (World Health Organization Multicentre Growth Reference Study Group and de Onis, 2006; World Health Organization Multicentre Growth Reference Study Group, 2006).

In 2011 the General Assembly of the United Nations announced the United Nations Decade of Action on Nutrition (2016–2025) to increase efforts to 'eradicate hunger and prevent all forms of

* Corresponding author.
E-mail addresses: johannes.seiler@nadel.ethz.ch, johannes.seiler@uibk.ac.at (J. Seiler), kenneth.harttgen@nadel.ethz.ch (K. Harttgen), tkneib@uni-goettingen.de (T. Kneib), stefan.lang@uibk.ac.at (S. Lang).

http://dx.doi.org/10.1016/j.ehb.2020.100950
1570-677X/

malnutrition worldwide' (United Nations, 2015). The highest shares of malnourished children are found in Asia and sub-Saharan Africa, and in 2016, 23.9% (Asia) and 31.2% (sub-Saharan Africa) of children were found to be stunted, and 9.9% and 7.4% were found to be wasted.[1] Globally, malnutrition is highly concentrated in these two regions, which account for 91% (92%) of the 149 (49) million stunted (wasted) children globally. Within these two continents the most affected sub-regions are South Asia, Eastern, Middle, and Western sub-Saharan Africa (World Health Organization, 2017; United Nations Children's Fund et al., 2017, 2019).

Assessing anthropometric measures and associated risk factors, while controlling for geographic factors, will help to evaluate and monitor the progress on Sustainable Development Goal 2, zero hunger, and in particular the second sub goal, which aims to end all forms of malnutrition by 2030. Identifying areas with high prevalence of low anthropometric outcomes can help to improve the provision of assistance for the population in need.

Studies that analyse anthropometric measures of malnutrition combining individual data and spatial information include Belitz et al. (2010), Kandala et al. (2011), Haile et al. (2016), and Gayawan et al. (2019). These studies apply geostatistical regression models to analyse spatial differences of malnutrition for individual countries in Asia and sub-Saharan Africa and aim to identify geographic hotspots with a high prevalence of malnutrition within the analysed country. However, studies which analyse determinants of malnutrition in combination with spatial information while jointly pooling several countries are scarce (see, for instance, Kandala et al., 2009; Osgood-Zimmerman et al., 2018). While growth failure and its socio-economic determinants are analysed by Kandala et al. (2009), explicitly accounting for spatial heterogeneity using Markov random fields for sub-national regions in three countries located in Eastern sub-Saharan African, the study by Osgood-Zimmerman et al. (2018) aims to map spatio-temporal trends of growth failures for the whole continent by taking advantage of the georeferenced survey data provided by the Demographic and Health Surveys (DHS). The latter approach has the advantage that the estimated effects are available on a finer resolution, which allows for the identification of areas with high growth failure prevalence beyond the administrative subdivisions within a country. Identifying these spatial hotspots can help to evaluate and monitor the progress towards the SDGs on a sub-national level. This is of particular importance for policymakers in order to distribute assistance more effectively within countries.

Our analysis examines effects of socio-economic correlates of malnutrition in combination with remote sensed data and spatio-temporal trends for long- and short- term nutritional deficiencies using the standard anthropometric measures that approximate chronic and acute undernutrition. The inclusion of remote sensed information in the analysis of growth failures is motivated by their increased availability and recent studies that highlight the importance of variables related to climate- (drought severity, rainfall), health- (malaria incidence), or population-dynamics (population density) for which remote sensed data products exist (see, for example, López-Carr et al., 2016; Bauer and Mburu, 2017; Amoah et al., 2018). The novel contributions to the literature on malnutrition are threefold: first, in this comprehensive study for sub-Saharan Africa and South Asia, we go beyond the existing literature by analysing spatio-temporal patterns of childhood malnutrition, while also controlling for underlying and basic determinants of malnutrition for a large sample from 38 low- and middle-income countries located in sub-Saharan Africa and South Asia for the period from 1990 to 2016. Combining data taken from the DHS and merging it with several other data sources allows us to add an economic, a political, a socio-economic, and an environmental perspective to our analysis on childhood malnutrition. For this we pool individual socio- economic characteristics stemming from the household recode section of available georeferenced DHS for more than one million children within sub-Saharan Africa and South Asia with remote sensed information from various different sources.

Second, by relying on Bayesian distributional regression in our analysis, we are able to model all parameters of the underlying response distribution.[2] Besides considering complex spatio-temporal interactions, and accounting for complex non-linear relationships, this approach explicitly allows us to model the mean μ and the standard deviation σ of the underlying response distribution, and we analyse the whole distribution accordingly. This is also helpful to gain more accurate results and better targeting of undernourished children as Osgood-Zimmerman et al. (2018) highlights small scale heterogeneity within and between sub-national boundaries.

Third, child malnutrition is analysed at the individual level, permitting us to include information on the child and household level to make better use of the United Nations Children's Fund (UNICEF) conceptual framework to assess malnutrition. For example, we explicitly account for potential gender differences, an observation highlighted in the literature. Moreover, relying on distributional regression models has the advantage that the effects of included covariates remain interpretable. Even though, these effects cannot be interpreted as causal given the data structure, the importance of a covariate can be interpreted. This is of great relevance for future studies in this area, that aim to establish a causal relationship.

Apart from the three major contributions, extending the existing literature on this important topic, this research has also limitations, which we want to acknowledge, before we briefly summarise our main findings. First, surveys such as the DHS report information on anthropometric measures only for those children living at the day of the interview. Accordingly, the analysis in this article and studies with a similar focus, for example the article by Osgood-Zimmerman et al. (2018), are restricted to the observable anthropometric measures of children who are still alive on the day of the interview. However, recent studies such as Alderman et al. (2011) or Harttgen et al. (2019) simulate the anthropometric status and in order to generate plausible values for the anthropometric measures of the whole population and deceased children. They do not find a statistically significant difference for the first group. Second, merging a large number of surveys and using the available observational data from the DHS does not allow us to draw causal conclusions. The effects found in this study are prone to a (potentially) large endogeneity bias and can only be seen as correlation between the anthropometric measures and the variables of interest.

Our results show strong non-linear effects of included socio-economic covariates, highlighting the importance of characteristics, such as maternal education or the family's wealth. Moreover, gender differences that have been highlighted in the literature (for

[1] Stunting refers to the height-for-age z-score and reflects long-term nutritional deficiencies, while wasting refers to the weight-for-height z-score and measures acute nutritional deficiencies. The z-score is calculated as follows: $z_i = \frac{x_i - x_{m,r}}{\sigma_r}$, where x_i is the anthropometric measurement of child i, $x_{m,r}$ is the median anthropometric index of the reference population, and σ_r is the standard deviation of the reference population. The z-score is calculated following the recommendations of the WHO growth standard (World Health Organization Multicentre Growth Reference Study Group, 2006).

[2] Choosing the response distribution of the anthropometric measures to be Gaussian, both parameters, the location parameter μ, and scale parameter σ are modelled. Of course also other response distributions can be incorporated.

Table 1
UNICEF framework of malnutrition: key factors of childhood malnutrition found in the literature and included in this analysis.

Variable	Description	UNICEF framework	Author	Data source	Anthropometric measure	Level	Relationship
Child specific factors							
Birth order	Binary index birth order fourth or higher	Underlying	Gayawan et al. (2019)	DHS Nigeria 2013	Stunting, underweight, wasting	Child	Fourth or higher in birth order significantly more stunted and underweight
Breastfeeding	Interaction breastfeeding interval and age of child	Underlying	Belitz et al. (2010)	National Family Health Survey (NFHS) India 1998/99	Stunting	Child	Poor nutritional status when breastfeeding interval ≤ six month
Age child	Age of children in month	–	Kandala et al. (2011)	DHS Congo, Dem., Rep. 2007	Stunting	Child	Non-linear decreasing
Age child	Age of children in month	–	Gayawan et al. (2019)	DHS Nigeria 2013	Stunting, underweight, wasting	Child	Nonlinear behaviour depending on analysed indicator
Gender	Binary indicator	–	Kandala et al. (2009)	DHS Malawi, Tanzania, Zambia 2009	Stunting	Child	Female children less stunted
Gender	Binary indicator	–	Kandala et al. (2011)	DHS Congo, Dem., Rep. 2007	Stunting	Child	Female children less stunted
Gender	Binary indicator	–	Gayawan et al. (2019)	DHS Nigeria 2013	Stunting, underweight, wasting	Child	Female children less stunted
Vaccination coverage	Child fully vaccinated	Underlying	Belitz et al. (2010)	NFHS India 1998/99	Stunting	Child	Higher z-score when child is fully vaccinated
	Immunisation rate	Underlying	Frongillo et al. (1997)	WHO Global Database on Child Growth	Prevalence of stunting, wasting	Country	Lower prevalence of wasting associated with higher immunisation rates
Household specific factors							
Household's wealth	Quantiles wealth index	Basic	Gayawan et al. (2019)	DHS Nigeria 2013	Stunting, underweight, wasting	Child	Nutrition improves with household's wealth
Household's wealth	Quartile wealth index	Basic	Vollmer et al. (2017)	DHS from 39 countries 1990–2014	Composite index of anthropometric failure	Child	Prevalence of anthropometric failure improves with household's wealth
Residency	Binary indicator	Underlying	Kandala et al. (2009)	DHS Malawi, Tanzania, Zambia 2009	Stunting	Child	Stunting worse in rural areas
Residency	Binary indicator	Underlying	Kandala et al. (2011)	DHS Congo, Dem., Rep. 2007	Stunting	Child	Stunting worse in rural areas
Residency	Binary indicator	Underlying	Gayawan et al. (2019)	DHS Nigeria 2017	Stunting, underweight, wasting	Child	Anthropometric measures worse in stunting areas
Maternal specific factors							
Age mother	Age of mother at birth	–	Gayawan et al. (2019)	DHS Nigeria 2013	Stunting, underweight, wasting	Child	Non-linear increasing for stunting and underweight, insignificant for wasting
Education mother	Female literacy rate	Basic	Frongillo et al. (1997)	WHO Global Database on Child Growth	Prevalence of stunting, wasting	Country	Improving with education
Education mother	Mother's level of educational attainment	Basic	Gayawan et al. (2019)	DHS Nigeria 2013	stunting, underweight, wasting	Child	Positive association with anthropometric measures
Education mother	Mother's level of educational attainment	Basic	Vollmer et al. (2017)	DHS from 39 countries 1990–2014	Composite index of anthropometric failure	Child	Prevalence of anthropometric failure improves with education
Environmental and socio-economic factors							
Wealth country	Gross national product	Basic	Frongillo et al. (1997)	WHO Global Database on Child Growth	Prevalence of stunting, wasting	Country	Lower prevalence of stunting associated with higher GNP levels
Wealth country	Gross domestic product	Basic	Smith and Haddad (2015)	WHO UNICEF	Prevalence of stunting	Country	Lower prevalence of stunting associated with higher GDP levels
Time trend	Pentads (1980–2005)	–	de Onis et al. (2000)	WHO Global Database on Child Growth and Malnutrition	Prevalence stunting, wasting	Region	Differing between regions, decreasing in most regions
Time trend	Pentads (1990–2020)	–	de Onis et al. (2012)	WHO Global Database on Child Growth and Malnutrition	Prevalence stunting, wasting	Region and countries	Differing between regions, decreasing in most regions
Spatial factors							
Rainfall	Precipitation	Basic	López-Carr et al. (2016)	DHS, CHIRPS	Stunting, wasting	Grid cell	Stunting improves with increasing rainfall
Vegetation index	Normalized difference vegetation index (NDVI)	Basic	Johnson and Brown (2014)	DHS of five countries in Western SSA 2001–2006	Severely stunted or wasted	Children	No association with stunting, higher NDVI reduces prevalence of wasting
Vegetation index	NDVI	Basic	López-Carr et al. (2016)	DHS, GIMMS	Stunting, wasting	Grid cell	Negative
Vegetation index	NDVI	Basic	Bauer and Mburu (2017)	IBLI Survey Kenya 2009–2013	MUAC	Children	Positive

Table 1 (*Continued*)

Variable	Description	UNICEF framework	Author	Data source	Anthropometric measure	Level	Relationship
Drought index	Aridity	Basic	Osgood-Zimmerman et al. (2018)	DHS, Malaria Atlas Project	Prevalence of stunting, underweight, wasting	Grid cell	Effect not further specified
Malaria	Plasmodium falciparum endemicity	Basic	Osgood-Zimmerman et al. (2018)	DHS, Malaria Atlas Project	Prevalence of stunting, underweight, wasting	Grid cell	Effect not further specified
Malaria	Plasmodium falciparum incidence	Basic	Amoah et al. (2018)	DHS, Malaria Atlas Project	Stunting	Grid cell	Weak association with both negative and positive effects depending on survey
Population density	Number of people per km^2	Basic	Osgood-Zimmerman et al. (2018)	DHS, WorldPop	Prevalence of stunting, underweight, wasting	Grid cell	Effect not further specified
Night-time light	Night-time light	Basic	Osgood-Zimmerman et al. (2018)	DHS, MODIS	Prevalence of stunting, underweight, wasting	Grid cell	Effect not further specified

Notes: Incomplete list of risk factors associated with growth failures analysed in existing works and their classification according to the UNICEF framework of malnutrition. Bold covariates indicate covariates included in the final model of this analysis. The other covariates are omitted due to high correlation with included covariates.

example in Kandala et al., 2009, 2011; Gayawan et al., 2019) are mapped for the analysed regions, showing smaller differences in South Asia. Surprisingly, incorporating remote sensed information turned out to be statistically insignificant when controlling for individual- and household-specific socio-economic characteristics. In terms of spatio-temporal developments, South Asia has achieved the greatest progress towards reducing chronic malnutrition; however, when compared to sub- Saharan Africa, acute malnutrition still remains high.

The remainder of the paper is organised as follows: Section 2, provides an overview of the data, its source, and the included covariates. Section 3 summarises the statistical method focusing on modelling the spatial effect. Section 4 depicts the results, and Section 5 closes with an outlook and concluding remarks.

2. UNICEF framework of malnutrition and data

2.1. UNICEF conceptual framework to assess malnutrition

A conceptual framework to assess malnutrition was developed by the UNICEF in 1990 (United Nations Children's Fund, 1990) and was further refined in subsequent years (Black et al., 2008, 2013; United Nations Children's Fund, 2013). It aims to extend the problem of malnutrition to a wider scope than a solely physiological characterisation (United Nations Children's Fund, 1990). Instead, it claims that such a framework should also reflect the household, the socio-economic, and the environmental dimensions of malnutrition. The framework characterises these aspects according to how they affect malnutrition, and can be grouped into the following determinants: immediate determinants of malnutrition, underlying determinants, and basic determinants. While data for underlying determinants (for example, food security within household, quality of care, and health environment) and basic determinants (for example, the household's endowment of resources, education, or the economic or social conditions of the country in which a household is located) are available from various sources, the immediate causes of malnutrition (dietary intake and health status) are seldom included, and hard to quantify with respect to the temporal dimension. In the following we give a brief summary of the UNICEF framework and the different determinants of malnutrition.

2.1.1. Immediate determinants

Following the framework introduced by UNICEF, immediate determinants of malnutrition are the caloric intake and health status of the child, and affect directly the child. Both dimensions can be seen as interrelated, as nutritional intake influences health status and vice versa. Information on immediate determinants, however, is not sampled routinely by the DHS, and would also require a different sampling mechanism – observing individuals over time – as both dimensions are subject to change.

2.1.2. Underlying determinants

Underlying determinants of undernutrition are household characteristics that impact the nutritional status of the individual child through their effect on the immediate determinants. These can be roughly grouped into three dimensions: First, the household's ability to guarantee food security for all household members, especially for all children within the household. Children growing up in a household that cannot attribute enough resources to provide and secure enough quality food on a daily basis are prone to various growth failures (Gayawan et al., 2019; Vollmer et al., 2017). Second, adequate maternal and child care. Third, adequate access to health services and the provision of a healthy environment for childhood development. For instance, pathogens that spread infectious disease such as malaria and a child is exposed to will impede the development of the child through transmitted infectious diseases. Accordingly, both the quality and the access to health services is crucial for the long-term development of children. Similarly, the environment in which a child is raised, and the household's sanitation facilities and access to water, are important factors associated with growth failures of children.[3] For instance Spears (2013) and Hathi et al. (2017), find that the two aforementioned factors are robust determinants which explain growth failures and child mortality. A recent study by Aizawa (2019) highlights that children growing up in

[3] To reduce the number of covariates and to speed up, the estimation the asset index also includes information on the households access to water and sanitation facilities. The index is calculated following Filmer and Pritchett (2001) and Sahn and Stifel (2003). This also increases the number of included surveys and the sample size as the wealth index of the household provided by the DHS (hv270) is not calculated based on a principal component analysis for all surveys.

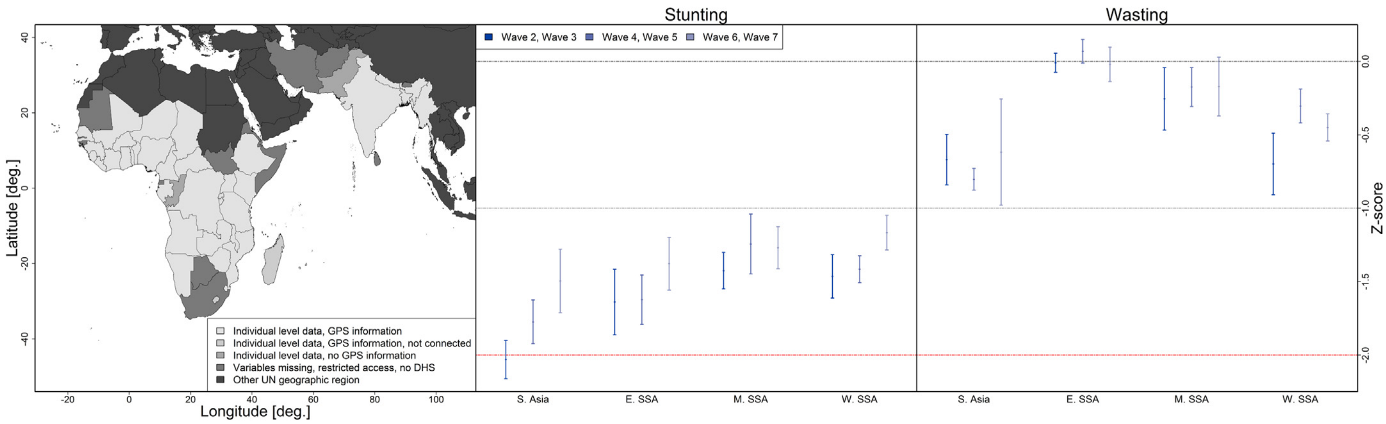

Fig. 1. Map of included countries, trend stunting and wasting by UN regions and survey wave with 95% confidence intervals. *Source:* DHS; calculations by the authors.

marginalised households that have poor access to sanitation facilities, or a low level of parental and maternal education, are more vulnerable to undernourishment. This study also argues, like Hatton et al. (2018), that family or household size is associated with growth failures, potentially through increasing competition for food in larger households. The latter study also establishes a negative causal effect of the family size on anthropometric outcomes.

2.1.3. Basic determinants

Basic determinants of malnutrition include aspects beyond the individual and household level, and consider potential regional, national or even global aspects of child malnutrition. Basic determinants add an economic, a political, a socio-economic, and an environmental perspective to the determinants of malnutrition and permit a closer look at malnutrition of children in a broader context (Smith and Haddad, 2015). López-Carr et al. (2016), for instance, finds a positive association between stunting and rainfall. Moreover, Smith and Haddad (2015) find that in economically more successful countries the prevalence of stunting and wasting is lower. Income at the country level is thought to influence childhood nutrition via two main channels: increasing income and pro-poor growth.

Table 1 summarises key findings found in the literature on childhood undernutrition of underlying and basic determinants, offers an overview of the effects one can expect from determinants of childhood malnutrition, and indicates socio-economic and remote sensed characteristics included in this analysis.

2.2. Anthropometric measures

Long-term nutritional deficiencies are approximated using the height-for-age z-score, also referred to as stunting, since it best reflects long-term development (World Health Organization, 1999). In contrast, short-term nutritional deficiencies, and accordingly, acute malnutrition, are detected by either measuring the mid-upper arm circumference (MUAC), examination for bilateral pitting oedema, or the weight-for-height z-score (wasting) (World Health Organization, 1999, 2013). The DHS provides information on the weight-for-height z-score, which is routinely recorded for children younger than five years. In this work we are modelling two anthropometric measures, stunting and wasting, which give a broad picture of malnutrition, and are derived from the children's recode of the DHS following the guidelines of the World Health Organization Multicentre Growth Reference Study Group (2006). They are the recommended indicators used to assess growth failures under the SDG (Schmidt-Traub et al., 2015).

2.3. Data source

2.3.1. Demographic and Health Surveys

The main data used in our analysis is sourced from the children's recode of each country's national DHS, for which either the GPS location of the primary sampling unit the household in which child i lives in resides, or information about the administrative region has been collected.[4] The DHS provides information about a country's population and the, socio-economic and health status of individuals, and i nationally representative and standardised across countries and over time. The data is collected by Macro International Inc., Calverton, Maryland and local administration and receives funding from U.S. Agency for International Development (USAID).

The study, depending on the analysed anthropometric measure, uses information from the DHS children's recode of 1,292,758 children sampled at 13,731 locations within 38 countries between 1990 and 2016.[5] Five of the included countries are located in South Asia and 33 are located in sub-Saharan Africa. This is shown in Fig. 1, where the left-hand panel shows the included countries, while the right-hand panel illustrates the improvements of the analysed anthropometric measures over time. See also Table B.1 for country details on the development of the anthropometric measures.

2.3.2. Remote sensed and further covariates

A vast literature focuses on the socio-economic aspects of health outcomes such as low anthropometric measures or mortality of children in developing countries, but do not consider remote sensed data (see, for instance, Black et al., 2013; Fenske et al., 2013; Kandala et al., 2011, 2014; Ayele et al., 2015; Smith and Haddad, 2015). For example, Smith and Haddad (2015) emphasise that, besides the educational level of the mother, access to drinking water, and sanitation, the country's GDP has a strong non-linear relationship with stunting, and this relationship is particularly pronounced for low-income countries. This body of literature aims to either find correlates of health outcomes or to establish causal relationships between socio-economic covariates and health outcomes, with the final goal of improving policy advice that yields improved health outcomes. Despite the interest in this topic,

[4] To include also surveys for which geographic information is only available in the form of the administrative region, the GPS coordinate of the regions centroid is used.

[5] Numbers presented in the text are for stunting, when instead wasting is used as measure of undernutrition the sample consists of 1,275,387 children sampled at 13,509 locations within 38 countries.

limited work on the influence of geophysical and environmental aspects on health outcomes has been conducted, in particular for malnutrition (see, for instance, Grace et al., 2012; Bauer and Mburu, 2017). This is mainly due to data limitations, however, and with changing ecosystems and environments due to climate change, health outcomes are potentially becoming increasingly affected by geophysical and environmental aspects. Combining individual and country level data with remote sensed data can therefore help formulate targeting practices to improve health outcomes such as growth failures and child mortality (Brown et al., 2014).

The data from the DHS is supplemented by additional socio-economic and remote sensed covariates that have been used in the literature, in addition to the standard socio-economic factors provided by the DHS to model growth failures using geophysical and environmental aspects. Previous country studies have linked various remote sensed data to growth failures. For example, Bauer and Mburu (2017) use the normalized difference vegetation index (NDVI) as a drought measure, and find a positive relationship between the NDVI and acute malnutrition, and as a consequence, the authors emphasise the negative effects of varying climate patterns on childhood malnutrition. However, other studies (see, for example, Johnson and Brown, 2014) find no clear association between the NDVI and chronic malnutrition. López-Carr et al. (2016) find a positive association of precipitation history on stunting, indicating the potential relevance of climate-specific factors. Similarly, night-time light data has drawn the attention of researchers who consider it to be, for example, a proxy for urbanisation or economic activity at sub-national levels (see, for instance, Savory et al., 2017). Accordingly, remote sensed covariates that reflect population dynamics (population density, urbanisation), environmental changes (for example changes in precipitation, temperature, the growing season), and economic development (e.g. level and growth of GDP) can be potentially useful in explaining variation in health outcomes. See Table A.1 for factors related to childhood malnutrition found in the literature. The covariates included in this analysis stem from different data sources. See Table A.1 for additional information on these covariates and their sources. In a recent work by Osgood-Zimmerman et al. (2018), growth failures are mapped using remote sensed information, although particular effects were not further specified. However, to our knowledge, no multi country study exists that analyses growth failures by combining socio-economic and remote sensed data. Going beyond the work of Osgood-Zimmerman et al. (2018), we merge individual level characteristics with remote sensed data, and analyse whether including remote sensed data provides additional information when accounting for children and household characteristics.

Individual- and household-level covariates, are merged with remote sensed covariates in a way that is similar to Grace et al. (2012). Remote sensed data is aggregated by including a buffer around the centroid of the grid cell a child pertains to, and

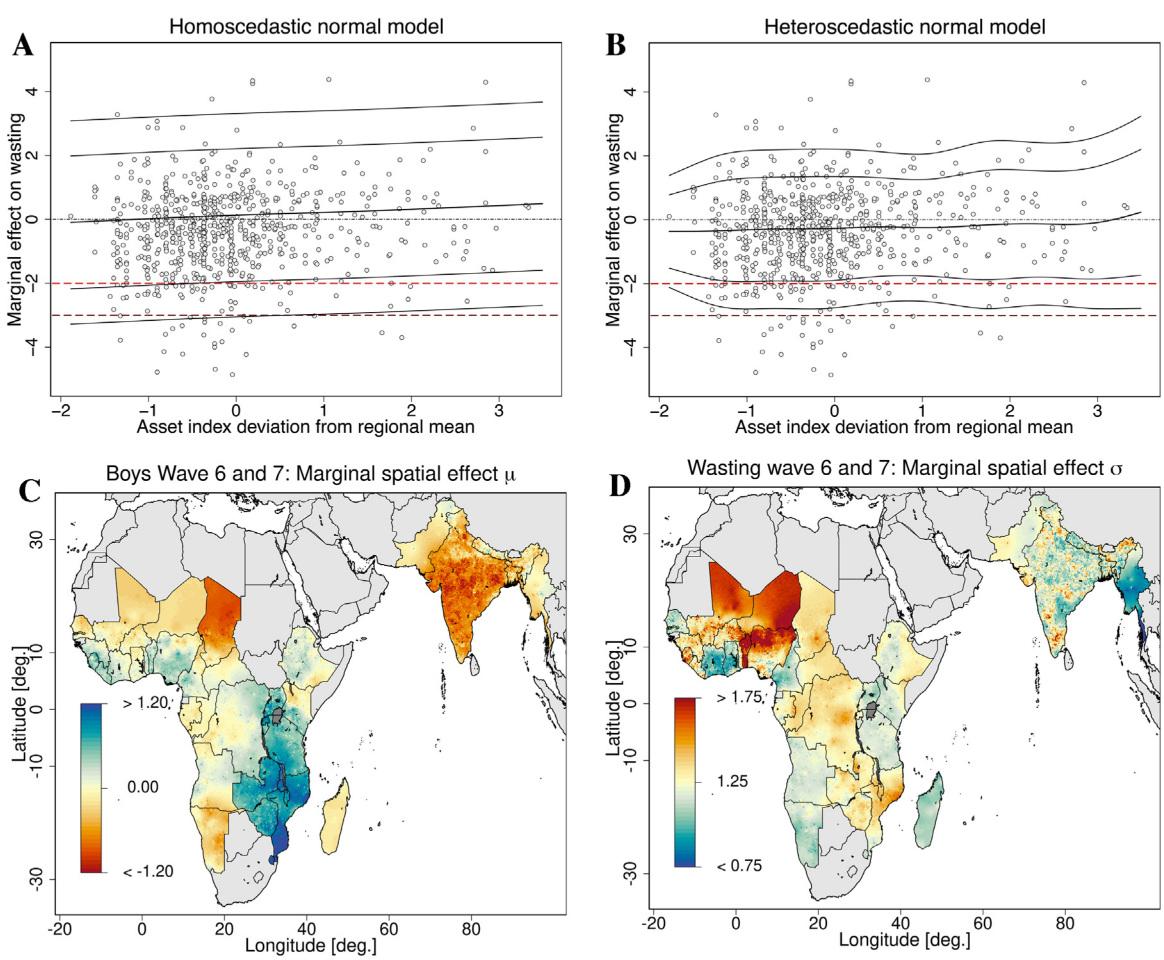

Fig. 2. Illustration of the homoscedastic Gaussian model (top left) as specified in Model 1 and heteroscedastic Gaussian model (top right) as specified in Model 6, together with a random sample drawn from the underlying data used to estimate both models. *Notes:* The panels show the estimated marginal effect of the asset index on the weight-for-height z-score together 2.5%, 10%, 90%, 97.5% quantiles. See Section 3 for a more elaborate model description. In the bottom panel the spatio-temporal distribution of the height-for-age z-score is depicted. *Source:* DHS; calculations by the authors.

Table 2
Estimated results for the mean μ of the categorical covariates.

Variable	Covariate	South Asia		Eastern SSA		MDG		Central SSA		Western SSA	
		Mean	95% CI	Mean	95% CI	Mean	95% CI	Mean	95% CI	Mean	95% CI
Stunting	Intercept	−1.91	−1.98; −1.86	−1.55	−1.6; −1.5	−1.91	−2.08; −1.75	−1.57	−1.67; −1.47	−1.59	−1.66; −1.5
	Male	−0.03	−0.04; −0.02	−0.09	−0.11; −0.08	−0.09	−0.15; −0.04	−0.08	−0.11; −0.06	−0.09	−0.1; −0.07
	Urban	0.01	0.01; 0.02	0.07	0.06; 0.08	−0.01	−0.04; 0.02	0.02	0.01; 0.04	0.08	0.07; 0.09
Wasting	Intercept	−0.76	−0.82; −0.7	−0.08	−0.12; −0.04	−0.46	−0.62; −0.31	−0.14	−0.22; −0.06	−0.32	−0.39; −0.25
	Male	−0.02	−0.03; −0.01	−0.01	−0.02; 0	−0.03	−0.09; 0.03	−0.02	−0.04; 0	−0.01	−0.03; 0
	Urban	0	−0.01; 0	0.01	0; 0.01	−0.06	−0.08; −0.03	−0.01	−0.02; 0.01	0	−0.01; 0

Notes: As pointed out amongst others by Lai et al. (2015), spatial correlation between sampled units or locations is interpreted differently when separated by land or by sea. Accordingly, Madagascar (MDG) was treated separately from main land sub-Saharan Africa. International country codes (ISO-3) are used as abbreviations. *Source:* DHS; calculation by authors.

aggregating remote sensed information of all cells included within this buffer. This accounts for the random displacement of the DHS sampling cluster where the child resides, and the fact that geophysical and environmental aspects outside of the household's immediate place of residence might also influence the decisions made by household members with respect to nutrition.

3. Modelling growth failures of children

Having described the data and the UNICEF framework to assess malnutrition in the previous section, in this section we illustrate the main concept of Bayesian distributional regression, which enables us to model all parameters of a response distribution and relate growth failures of children to underlying and basic determinants of malnutrition. The idea of a distributional regression model is also illustrated in Fig. 2, which shows the advantages of modelling both the mean μ and the standard deviation σ using a heteroscedastic Gaussian model compared to the homoscedastic Gaussian model. In particular, this approach makes it possible to extend the analysis beyond the conditional mean. In the context of analysis of growth failures, this is of great importance, as (severe) growth failures of children are defined having a z-score below -2 (-3), emphasising the need to extend the analysis to more extreme quantiles. The first row illustrates the differences between the homoscedastic Gaussian model on the left and the heteroscedastic Gaussian model on the right, showing, for example, that the variation is lowest for small values of the explanatory variable. In addition, the spatio-temporal distribution of the weight-for-height z-score is shown in the second row, highlighting the high sub-national heterogeneity.

Bayesian hierarchical distributional regression is used to model the standard anthropometric indicators for each geographic region that belong to those most affected by low anthropometric indicators of children.[6] Accordingly, we model all parameters of the underlying response distribution, instead of only considering the conditional mean. This is crucial for more accurate results and better targeting of undernourished children as previous literature emphasises the high heterogeneity even within sub-national administration boundaries.

In this paper, we use distributional structured additive regression models that allows us to incorporate the following concepts that go beyond a classical regression approach:

- The estimation of all parameters of the response distribution: Assuming the anthropometric measure is normally distributed, both the mean and the standard deviation are related to a structured additive predictor.
- Complex spatio-temporal trends: Spatio-temporal heterogeneity is accounted for by including a smooth spatio-temporal effect.
- Non-linear relationships: Continuous covariates are estimated using Bayesian penalized splines (P-splines) to allow for complex non-linear covariate effects.
- Complex covariate interactions: Consider the age of the mother and the birth order of the child within the household, two highly correlated covariates. For example, the effect of being the third born within the household should vary for different ages of the mother, which makes it necessary to incorporate a two-dimensional effect.

3.1. Distributional regression

Bayesian structured additive distributional regression allows us to estimate all parameters of the response distribution (Klein et al., 2015a,b). Assuming that the response distribution for each indicator is Gaussian, both parameters of the normal distribution, the mean and the standard deviation, are related to a predictor of the regression containing socio-economic characteristics of individuals and spatial information at the cluster level. Thus, each indicator within a specific region is specified as Gaussian response, with $\texttt{z}-\texttt{score}_{il} \sim N(\mu_{il}, \sigma_{il})$.[7] Here $i = 1, \ldots, I$ indexes the observed children's within each region, and $l = 1, \ldots, L$ indexes the location of the grid cells within each geographical region the individuals pertain to. Accordingly, the regression model for each region and indicator can be specified as follows:

$$\begin{aligned} \boldsymbol{\mu} &= h_\mu(\boldsymbol{\eta_\mu}) &= \mathrm{id}(\boldsymbol{\eta_\mu}), \\ \boldsymbol{\sigma} &= h_\sigma(\boldsymbol{\eta_\sigma}) &= \exp(\boldsymbol{\eta_\sigma}), \end{aligned} \quad (1)$$

where the response functions h_μ and h_σ link μ and σ to structured additive predictors using the corresponding link function, and the predictors can contain a different set of covariates. Choosing the appropriate link function guarantees that the restrictions of the parameter space are satisfied (see also methodology manual of **BayesX**, Belitz et al., 2015). See Appendix C for a more thorough discussion on Bayesian distributional regression.

For estimation the open source statistical software **BayesX** (Belitz et al., 2015) is used, and the data has been pre-processed using the statistical software **R** (R Core Team, 2016) and the

[6] These regions are South Asia, Eastern, Middle, and Western sub-Saharan Africa. Sub-Saharan Africa is divided into its three UN regions (Eastern, Middle, Western), which allows for different covariate effects, while avoiding the tremendous increase in computational time and memory which accompanies further division into smaller regions. In addition, as structured additive regression models require that the map object is connected, stunting and wasting was estimated separately for Madagascar.

[7] Choosing the response distribution to be Gaussian can be justified by verifying the histograms of the response variables. Further analysis using randomised quantile residuals as suggested by Dunn and Smyth (1996) confirms the normal distribution to be an appropriate choice. See also D for details.

corresponding **R**-packages **bamlss** (Umlauf et al., 2018a), **BayesX** (Umlauf et al., 2018b) and **R2BayesX** (Umlauf et al., 2015). The spatial effects are visualised relying on a diverging hue-chroma-luminance (HCL) colour space to allow for effective visualisation using the **R**-package **colorspace** (Zeileis et al., 2009).

4. Results

Table 2 summarises the effects of the covariates which enter the model linearly – the place of residence and the gender – both of which are found to be significant and in line with the literature (see Table 1 for established effects found in the literature). The difference between boys and girls for both anthropometric measures is found to be lowest in South Asia, where the anthropometric measures are 0.03 and 0.02 standard deviations lower for boys, respectively. This potentially reflects the observed gender preferences for boys in South Asia, observed by for instance Arnold (1997) and Dancer et al. (2008), and accordingly the unequal distribution of the households resources.

4.1. Socio-economic characteristics

Figs. 3 and 4show the results for a selection of the included continuous covariates which best describe the non-linear effects and the effect of the interaction caused by highly correlated covariates. Fig. 3 illustrates the marginal effects by region together with 10%, 30%, 70%, and 90% quantiles of the asset index, the years of education of the mother, and the year of the survey. Fig. 4 depicts the marginal effect on the mean μ and the standard deviation σ of the interaction between the age of the child and the breastfeeding duration, and the interaction of the age of the mother and the birth order.

Beginning with the asset index, a similar effect is found across the five analysed regions, which is that the nutritional status increases with the wealth of the household (reflected by the household's asset index). Similarly, as seen in the bottom panel of Fig. 3, the height-for-age z-score increases with the education of the mother. This increase is non-linear, however, with the steepest effect for the children of mother's with a high level of education. This implies that investment in education not only reduces child mortality (Breierova and Duflo, 2004; Grépin and Bharadwaj, 2015; Makate and Makate, 2016) but also decreases the chance of growth failures. This can be explained as follows: higher education results in monetary leverage and increases the income of the household through better job opportunities. In addition, women with a higher level of education can in some cases better assess the needs of their children, which will be reflected in the health status of the children. In addition, the results show the large dispersion present in the data, and emphasise the importance of modelling more than just the conditional mean.

Another finding is illustrated in the third and fourth row of Fig. 4, showing the effect of the age of the child and the breastfeeding duration on the anthropometric measure. Newborn children are better nourished, implying that children are not born undernourished and that environmental factors during pregnancy do not cause children to be born with anthropometric failures. The anthropometric status declines quickly until the age of approximately 12 months, after which the effect stabilises at a low level.

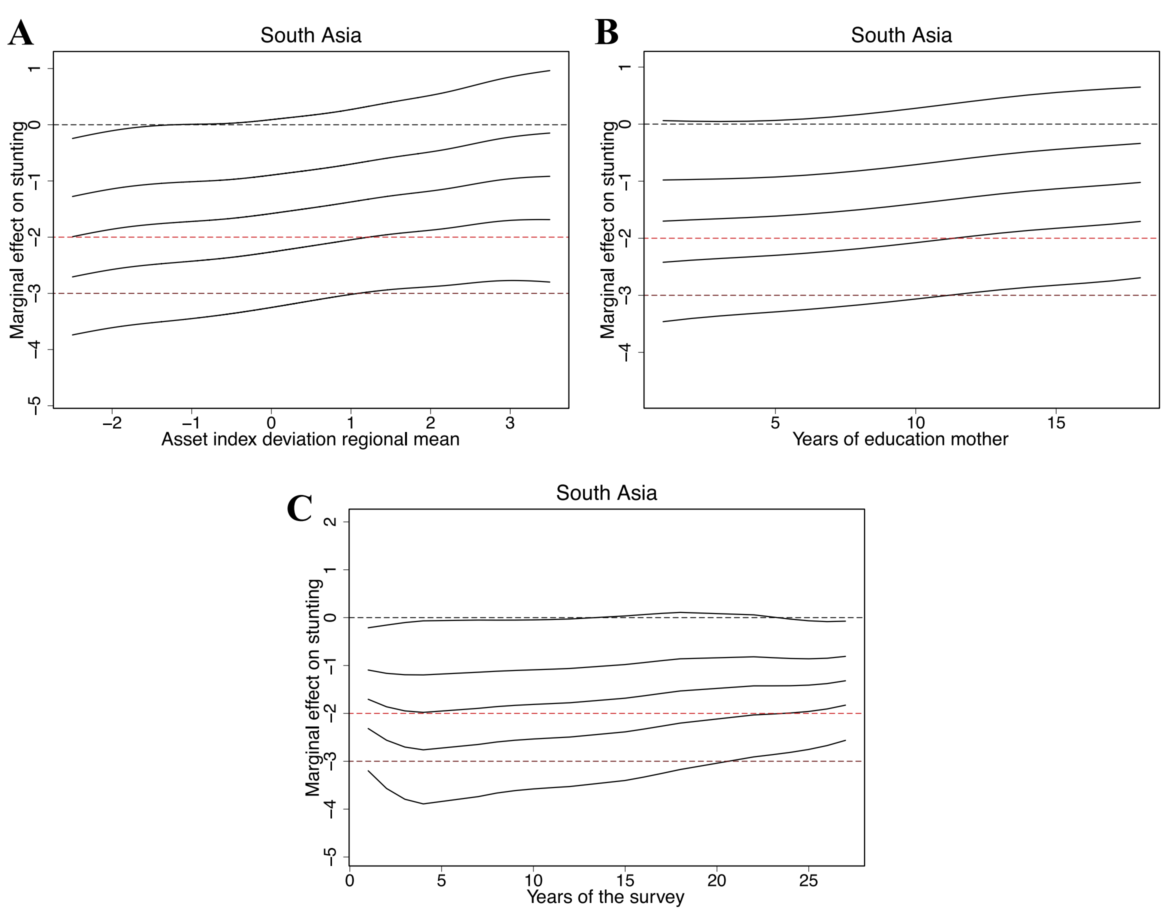

Fig. 3. Marginal effects on the height-for-age z-score of the asset index (first column), the years of education of the mother (second column), and the year of the survey (third column), together with the 10%, 30%, 70% and 90% quantiles for South Asia, Eastern sub-Saharan Africa, Madagascar, Central sub-Saharan Africa, and Western sub-Saharan Africa. *Source:* DHS; calculations by the authors.

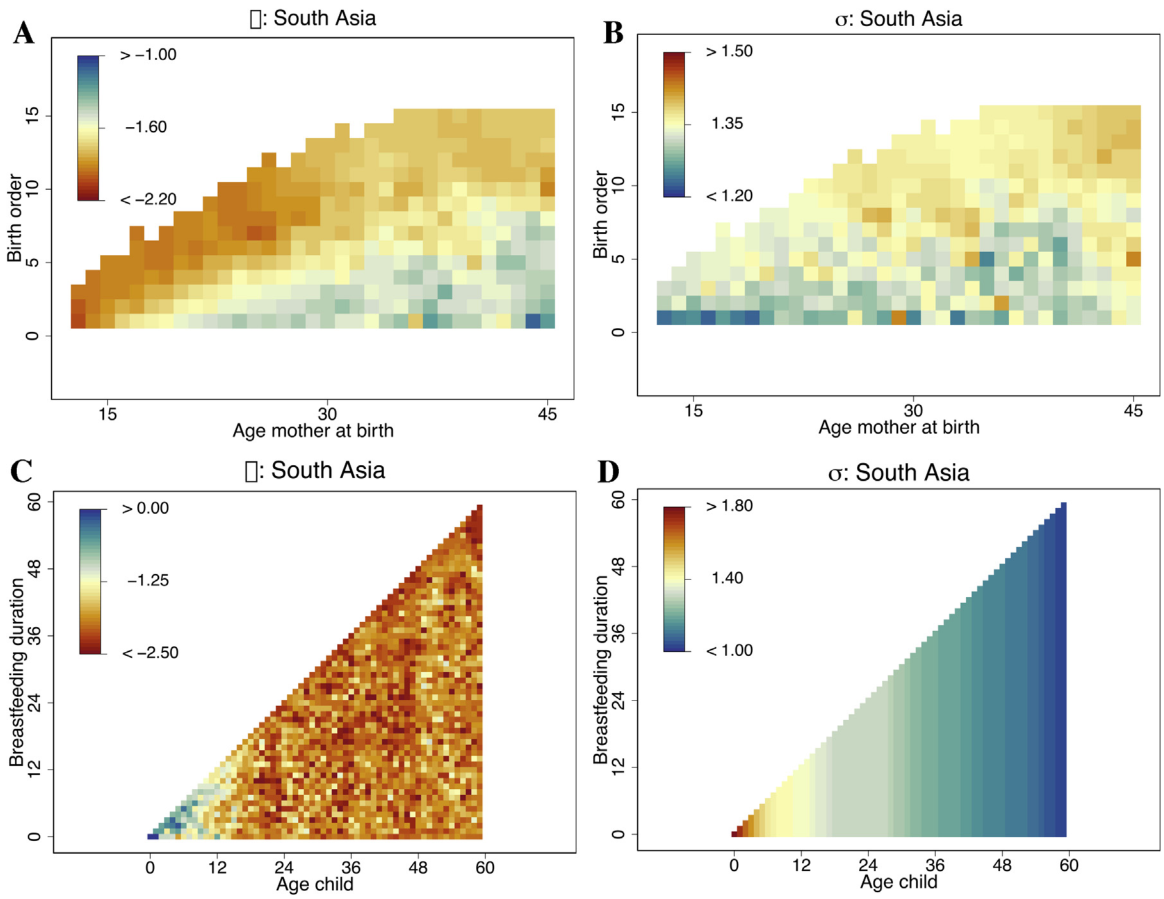

Fig. 4. Marginal effects on the height-for-age z-score for the interaction of the age of the mother and the birth order of the child (top), and the interaction of the age of the child and breastfeeding duration (bottom) for South Asia, Eastern sub-Saharan Africa, Madagascar, Central sub-Saharan Africa, and Western sub-Saharan Africa. *Notes:* The even lines of the panel show the marginal effects on the mean μ, while the odd lines of the panel show the marginal effect on the standard deviation σ. Note that the colour range differs due illustration purposes. *Source:* DHS; calculations by the authors (For interpretation of the references to colour in this figure legend, the reader is referred to the web version of this article.).

However, this effect also depends on breastfeeding duration. The children showing the lowest anthropometric outcomes are around three to four years old with an equally long breastfeeding duration. This effect is particularly dominant in Central and Western sub-Saharan Africa. This emphasises that breastfeeding duration and the age of the child cannot be interpreted as isolated factors. Similarly, the age of the mother and the birth order cannot interpreted individually given their high correlation.

4.2. Georeferenced information

Surprisingly, remote sensed information turned out to be statistically significant only when individual and household socio-economic characteristics were omitted. This is surprising as previous studies have found significant effects of remote sensed information, albeit without considering the effect of socio-economic covariates (Osgood-Zimmerman et al., 2018), or only considering their effects on a highly local level (López-Carr et al., 2016; Johnson and Brown, 2014). This aspect is also reflected in the significant increase of the DIC and WAIC of the models omitting individual characteristics (see Table C.1).

4.3. Spatio-temporal development

Spatial patterns of malnutrition are illustrated by overlying the map of South Asia and sub-Saharan Africa with the marginal spatial effect of the corresponding time. Fig. 5 illustrates the results for μ and σ for the height-for-age z-score. The first row shows the marginal spatio- temporal effect of boys, followed by the marginal spatio-temporal effect for girls, and the marginal effect of the standard deviation σ. Similarly, the marginal spatio-temporal effect for the weight-for-height z-score is depicted in Fig. 6.

While both indicators improved over time, differences between regions are striking. While the greatest progress on the height-for-age z-score, a measure of chronic malnutrition, was achieved in South Asia, progress seems to have stagnated and only to have improved after the fifth wave of the DHS in sub- Saharan Africa, in particular in Madagascar and within Western sub-Saharan African countries in Northern Nigeria, Southern Niger, and Central Chad, and in Eastern sub-Saharan Africa along the Great Rift Valley in North-Eastern Zambia, Burundi, and Tanzania. This is also consistent with findings of Akombi et al. (2017). Hotspots of chronic malnutrition are now concentrated in smaller areas within sub-Saharan Africa and South Asia, with the exception of Madagascar, which is found to belong to countries with the highest prevalence of chronic malnutrition, in line with findings of Rakotomanana et al. (2017). In addition to the improvement of chronic malnutrition, an increase in uncertainty can be observed, in particular in Western sub-Saharan Africa. This shows that growth failures still exist and that the positive development is accompanied by an increasing heterogeneity otherwise not captured by standard mean models.

In contrast, the weight-for-height z-score, a measure of acute malnutrition, seems to have stagnated in South Asia, while only

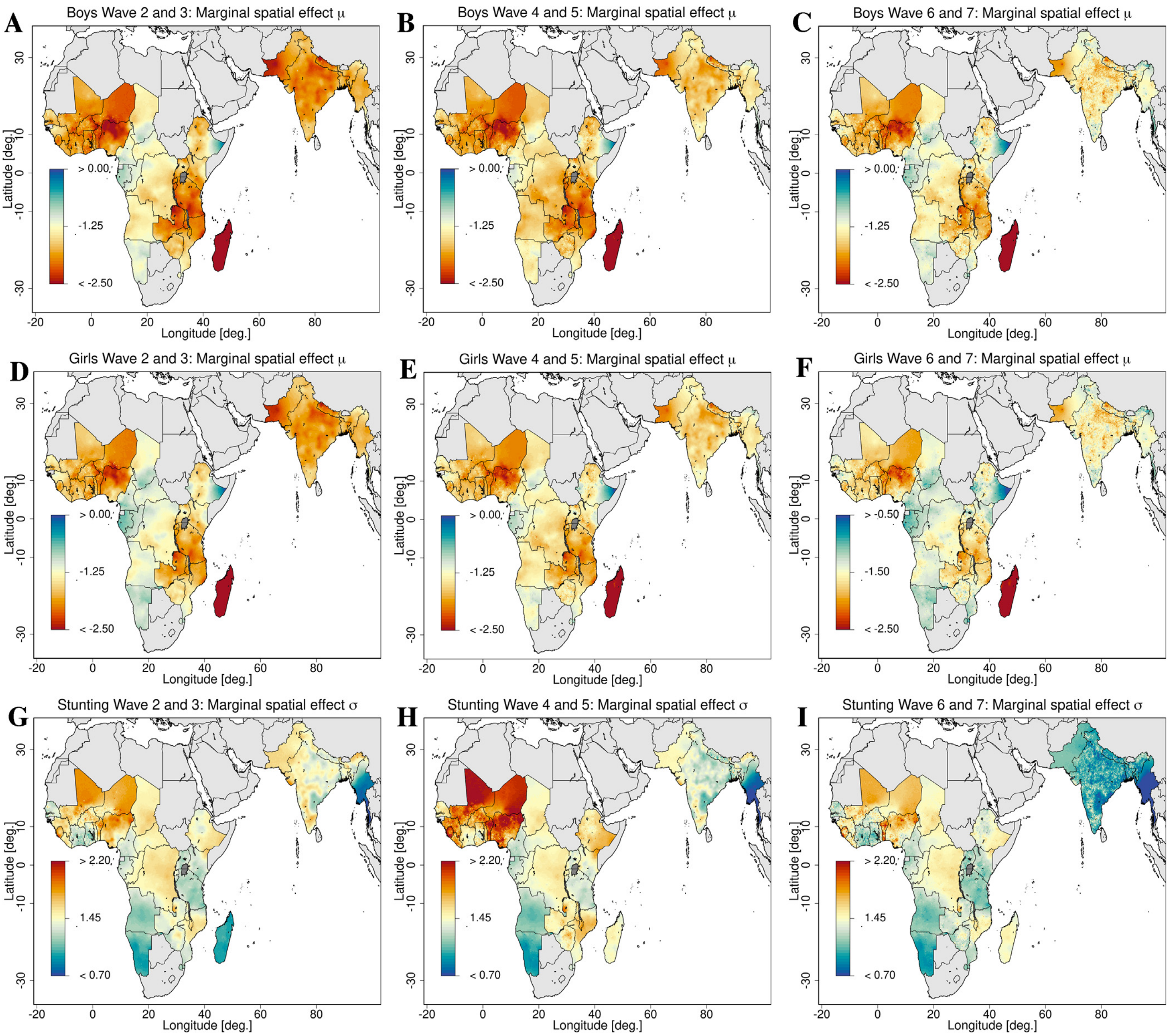

Fig. 5. Spatio-temporal distribution of the height-for-age z-score for the mean μ and the standard deviation σ over time. *Notes:* The top panel shows the marginal effects for the mean of the height-for-age z-score of boys, the middle panel shows the marginal effects for the mean of the height-for-age z-score of girls, while the bottom row shows the marginal effect for the standard deviation of the height-for-age z-score. The other covariates are kept constant at their means. *Source:* DHS; calculations by the authors (For interpretation of the references to colour in this figure legend, the reader is referred to the web version of this article.).

slowly improving in sub-Saharan Africa. When compared to chronic malnutrition, the levels of acute malnutrition are generally lower, though, hotspots exist in Madagascar, Southern Niger, Northern Nigeria and India.

5. Conclusion

The contribution of this work to the analysis of the MDGs and SDGs is twofold: first, risk factors associated with growth failures are analysed for a large sample of low- and middle-income countries located in sub-Saharan Africa and South Asia, paying particular attention to the spatio-temporal development of growth failures. This contributes to the monitoring of the SDGs. Second, high risk areas with particularly low anthropometric outcomes are identified, which can help improve the provision of assistance in severely affected areas. While all regions made improvements in reducing the levels of both acute and chronic malnutrition, our analysis shows that hotspots with high prevalence rates still exist, in particular for the height-for-age z-score. Of these regions, Madagascar has one of the highest observed prevalence rates for stunting (for a more in-depth analysis of the determinants of stunting in Madagascar, consult Rakotomanana et al., 2017). On a smaller scale, local hotspots of low height-for-age z-scores are found, for example, along the Great Rift Valley in North-Eastern Zambia, Burundi, and Tanzania and in Western sub-Saharan Africa in Northern Nigeria, and Central Chad, which are in line with the country-level findings of Akombi et al. (2017).

Using Bayesian hierarchical distributional regression, the effect of socio-economic and remote sensed data on anthropometric measures is estimated. In addition, the spatio-temporal development of malnutrition is analysed, identifying past, and current hotspots of low anthropometric outcomes of children of less than five years of age. Using Bayesian distributional regression to model heterogeneity highlighted in the literature (Osgood-Zimmerman et al., 2018) allows to account for sub-national heterogeneity and evaluate the uncertainty of our estimates.

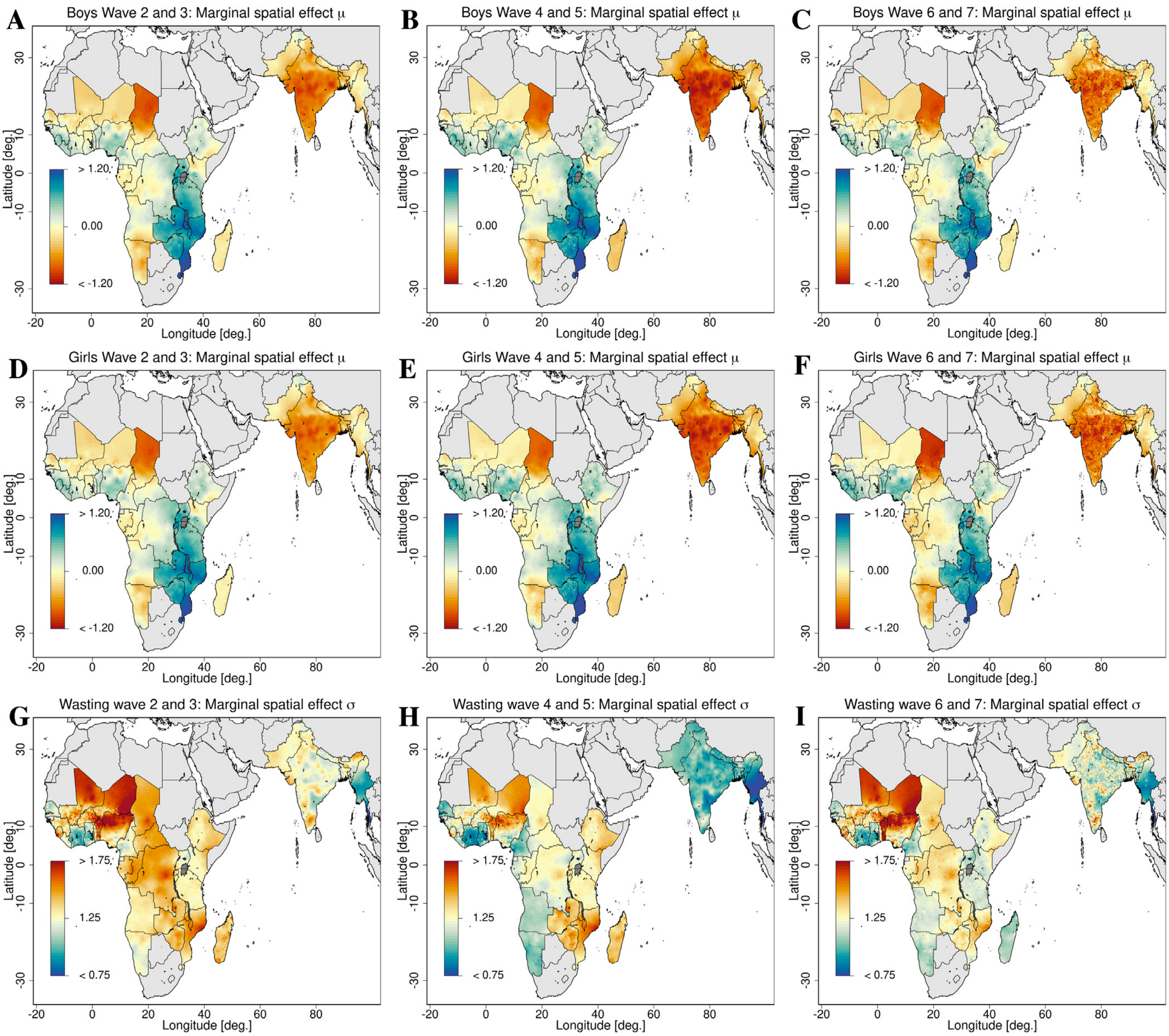

Fig. 6. Spatio-temporal distribution of the weight-for-height z-score for the mean and the standard deviation over time. *Notes:* The top panel shows the marginal effects for the mean of the weight-for-height z-score of boys, the middle panel shows the marginal effects for the mean of the weight-for-height z-score of girls, while the bottom row shows the marginal effect for the standard deviation of the weight-for-height z-score. The other covariates are kept constant at their means. *Source:* DHS; calculations by the authors (For interpretation of the references to colour in this figure legend, the reader is referred to the web version of this article.).

Most interestingly, while South Asia has made great progress in reducing chronic malnutrition, wasting is found to have increased. Moreover, large disparities on a sub-regional level exist, which emphasises the need to account for this heterogeneity. Mapping the results of the distributional regression approach allows us identify two points which remained unaddressed: first, it seems that disparities increase over time, which implies that even though anthropometric measures have improved on average, variation at the individual level has increased, and the gap between well- and undernourished children has become wider. This emphasises the importance of identifying the impact of socio-economic, environmental, and geophysical covariates on anthropometric measures. Second, it was found that children were better nourished and had better anthropometric outcomes (when considering chronic malnutrition) in the South-Western area of Zambia (subsistence farming) compared to North-Eastern areas of Zambia (mining), despite the fact that jobs in the mining business generate higher income. This could potentially be explained by the higher levels of pollution associated with mining regions, a possibility that calls for further research.

Author contributions

Johannes Seiler: Data curation, conceptualization, methodology, writing, reviewing, and editing. Kenneth Harttgen: Data curation, conceptualization, methodology, writing, reviewing, and editing. Thomas Kneib: Data curation, conceptualization, methodology, writing, reviewing, and editing. Stefan Lang: Data curation, conceptualization, methodology, writing, reviewing, and editing.

Declarations of interest

None.

Funding

Thomas Kneib received financial support from the German Research Foundation (DFG)within the research project KN 922/9-1. Johannes Seiler acknowledges financial support from the University of Innsbruckthrough a postdoctoral scholarship.

Declaration of Competing Interest

The authors report no declarations of interest.

Acknowledgements

The computational results presented have been achieved (in part) using the HPC infrastructure LEO of the University of Innsbruck. We thank Macro International Inc., for collecting the DHS and providing access to the data and Catherine Laflamme and Bartlomiej Kudrzycki for proofreading the manuscript.

Appendix A. Source geospatial covariates

Table A.1
Source additional covariates.

Covariate	Description	Resolution	Source	Reference
GDP	real per capita GDP	Country level	PENN World Table	Feenstra et al. (2015)
Malaria	Plasmodium vivax endemicity	30 arc sec. (~0.0083 deg.)	Malaria Atlas Project	Gething et al. (2012)
Night-time light	DMSP-OLS night-time Lights	30 arc sec. (~0.0083 deg.)	NOAA Earth Observation Group	National Geophysical Data Center (n.d.)
Night-time light	DMSP-OLS and VIIRS night-time Lights	30 arc sec. (~0.0083 deg.)	Harmonized NTL	Li et al. (2020)
Population density	Number of people per km^2; 1990–1999 GPWv3	2.5 arc min. (~0.04167 deg.)	Socioeconomic Data and Applications Center	Center for International Earth Science Information Network – CIESIN – Columbia University (and Centro Internacional de Agricultura Tropical – CIAT, 2005)
Population density	Number of people per km^2; 2000–2017 GPWv4	2.5 arc min. (~0.04167 deg.)	Socioeconomic Data and Applications Center	Center for International Earth Science Information Network – CIESIN – Columbia University (2017)
Self-calibrating Palmer Drought Severity Index (scPDSI)	scPDSI CRU4.03	0.5 deg.	Climate Research Unit	van der Schrier et al. (2013), Barichivich et al. (2018)

Notes: Source of additional covariates, including description, periodicity, source, and spatial resolution. Bold covariates have been included in the final model. As mentioned in footnote eight, the night-time light index has been omitted due to the high correlation with population density and as it contains, especially in sub-Saharan Africa many zeros.

Appendix B. Summary statistics data

B.1 Z-scores, and observations by country and survey year

Table B.1
Stunting, wasting and number of observations (*n*), by country, and survey year.

Country	Year	Stunting	*n*	Wasting	*n*	Country	Year	Stunting	*n*	Wasting	*n*	Country	Year	Stunting	*n*	Wasting	*n*
AGO	2016	−1.21	5749	−0.73	5842	IND	1999	−1.75	50,023	−1.51	51,307	NPL	2016	−1.07	3402	−0.98	3421
BDI	2010	−2.02	4898	−1.3	4927	IND	2006	−1.48	78,358	−1.47	80,197	PAK	1991	−2.04	5333	−1.47	5391
BDI	2016	−1.72	5153	−1.14	5150	IND	2015	−1.32	171,218	−1.47	173,501	PAK	2013	−1.65	6135	−1.17	6627
BEN	1996	−1.5	1248	−1.27	1277	KEN	1993	−1.56	6325	−0.91	6541	RWA	1992	−2	6292	−1.16	6359
BEN	2001	−1.51	5479	−1.12	5521	KEN	1998	−1.34	4150	−0.66	4308	RWA	2000	−1.65	9257	−0.92	9340
BEN	2006	−1.73	16,533	−0.98	17,424	KEN	2003	−1.31	7541	−0.72	7757	RWA	2005	−1.92	4773	−0.95	4849
BEN	2012	−1.77	13,775	−0.79	15,067	KEN	2009	−1.3	7769	−0.75	7966	RWA	2010	−1.61	6381	−0.69	6412
BFA	1993	−1.3	6339	−1.14	6556	KEN	2014	−1.11	14,546	−0.65	14,666	RWA	2015	−1.51	5994	−0.53	6042
BFA	1999	−1.67	5567	−1.46	5721	LBR	2007	−1.44	5812	−0.91	5933	SEN	1993	−1.41	4818	−1.06	4881
BFA	2003	−1.55	11,541	−1.44	11,748	LBR	2013	−1.19	4813	−0.79	4866	SEN	2005	−0.93	3815	−0.86	3862
BFA	2010	−1.29	9043	−1.18	9129	MDG	1992	−2.2	6504	−1.52	6519	SEN	2011	−1.2	5127	−0.99	5286
BGD	1997	−2.12	9242	−1.91	9618	MDG	1997	−2.04	4752	−1.44	4812	SEN	2013	−0.93	8244	−0.91	8216
BGD	2000	−1.9	11,443	−1.65	12,428	MDG	2004	−1.86	8076	−1.39	8221	SEN	2014	−1.03	8064	−0.87	8021
BGD	2004	−1.84	12,897	−1.68	13,157	MDG	2009	−1.6	8002	NA	NA	SEN	2015	−1.08	8057	−1	8050
BGD	2007	−1.63	11,930	−1.64	12,254	MLI	1996	−1.3	6144	−1.57	6100	SEN	2016	−0.95	8374	−0.93	8365
BGD	2011	−1.47	16,254	−1.44	16,645	MLI	2001	−1.53	9474	−1.26	9494	SLE	2008	−1.25	3355	−0.66	3459
BGD	2014	−1.3	10,479	−1.28	10,887	MLI	2006	−1.34	15,067	−1.18	15,194	SLE	2013	−1.2	7167	−0.6	7523
CAF	1995	−1.54	3465	−1.1	3520	MLI	2013	−1.34	6581	−1.16	6798	SWZ	2007	−1.2	4042	−0.23	4098
CIV	1994	−1.21	4533	−0.94	4544	MMR	2015	−1.09	1696	−0.92	1781	TCD	1997	−1.57	5887	−1.37	5991
CIV	2012	−1.18	5037	−0.82	5093	MOZ	1997	−1.56	5011	−1.01	5077	TCD	2004	−1.35	4835	−1.18	4892
CMR	1991	−1.36	1179	−0.67	1174	MOZ	2003	−1.77	12,099	−0.91	12,299	TCD	2015	−1.5	11,995	−1.31	12,200
CMR	1998	−1.24	1978	−0.61	2050	MOZ	2011	−1.57	15,328	−0.71	15,625	TGO	1998	−1.24	4552	−1.18	4591
CMR	2004	−1.24	5429	−0.5	5573	MWI	1992	−2.05	4704	−0.97	4787	TGO	2014	−1.29	4367	−0.98	4397
CMR	2011	−1.15	8229	−0.48	8329	MWI	2000	−1.95	14,247	−0.99	14,775	TZA	1992	−1.97	10,172	−1.19	10,367
COD	2007	−1.51	4633	−1.02	4979	MWI	2004	−2	12,293	−0.91	13,117	TZA	1996	−1.91	5117	−1.17	5176
COD	2014	−1.5	10,932	−1.02	11,126	MWI	2010	−1.85	6961	−0.81	7175	TZA	1999	−1.93	2786	−1.2	2813
COG	2005	−1	7239	−0.52	7400	MWI	2015	−1.17	4995	−0.53	5056	TZA	2005	−1.88	6910	−1.04	6963
COG	2012	−1.05	5827	−0.72	5861	NAM	1992	−1.34	5050	−0.96	5034	TZA	2010	−1.64	8457	−0.92	8588
ETH	2000	−1.97	13,085	−1.58	13,310	NAM	2000	−1.11	5293	−0.93	5370	TZA	2015	−1.04	5724	−0.51	5762

Table B.1 (*Continued*)

Country	Year	Stunting	n	Wasting	n	Country	Year	Stunting	n	Wasting	n	Country	Year	Stunting	n	Wasting	n
ETH	2005	−1.62	5377	−1.27	5698	NAM	2007	−1.1	7075	−0.84	7139	UGA	1995	−1.69	6894	−0.98	6987
ETH	2011	−1.56	14,095	−1.29	14,314	NAM	2013	−0.94	3470	−0.66	3461	UGA	2001	−1.74	6033	−0.91	6202
ETH	2016	−0.85	8213	−0.8	8394	NER	1992	−1.67	4912	−1.53	5012	UGA	2006	−1.45	2938	−0.86	2965
GAB	2000	−1.12	6209	−0.52	6239	NER	1998	−1.73	5026	−1.76	5082	UGA	2011	−1.13	1660	−0.68	1684
GAB	2012	−1.08	4505	−0.46	4624	NER	2006	−1.97	4538	−1.54	4628	UGA	2016	−0.93	3881	−0.46	3903
GHA	1993	−1.31	2465	−1.09	2481	NER	2012	−1.57	5686	−1.57	5841	ZMB	1992	−1.86	7756	−1.11	7854
GHA	1998	−1.32	3865	−1.08	3932	NGA	1990	−1.84	216	−1.33	218	ZMB	1996	−1.94	8757	−1.04	8912
GHA	2003	−1.38	4966	−0.95	5138	NGA	1999	−1.89	2587	−0.52	3337	ZMB	2002	−2.04	8717	−1.16	8955
GHA	2008	−1.07	3675	−0.73	3852	NGA	2003	−1.52	6786	−1.06	7031	ZMB	2007	−1.6	8048	−0.77	8334
GHA	2014	−0.96	4294	−0.74	4296	NGA	2008	−1.41	27,692	−0.96	30,199	ZMB	2014	−1.47	18,146	−0.81	18,599
GIN	1999	−1.21	5406	−0.88	5521	NGA	2013	−1.16	35,944	−1.11	37,279	ZWE	1994	−1.07	3839	−0.54	3856
GIN	2005	−1.45	3417	−0.99	3464	NPL	1996	−2.02	6225	−1.65	6560	ZWE	1999	−1.08	5422	−0.55	5599
GIN	2012	−0.97	4918	−0.82	4945	NPL	2001	−2.1	11,113	−1.71	11,224	ZWE	2006	−1.38	8254	−0.63	8694
GMB	2013	−1.17	2841	−1.08	2985	NPL	2006	−1.82	10,107	−1.6	10,183	ZWE	2011	−1.39	8882	−0.68	9025
IND	1993	−2.03	65,351	−1.77	84,931	NPL	2011	−1.58	5314	−1.32	5344	ZWE	2015	−0.89	5843	−0.23	5914

Notes: International country codes (ISO-3) are used as abbreviations. *Source:* DHS data sets; calculation by authors.

B.2 Descriptive statistic

Table B.2
Descriptive statistics of covariates.

Definition covariate	South Asia			Eastern SSA			MDG			Central SSA			Western SSA		
	Mean, %	SD	n	Mean, %	SD	n	Mean, %	SD	n	Mean, %	SD	n	Mean, %	SD	n
Age children (months)	25.61	16.24	486,520	26.83	16.92	347,765	26.59	17.03	27,334	26.82	17.15	108,979	27.46	17.19	322,160
Breastfeeding duration (months)	16.1	11.72	486,520	13.44	9.65	347,765	15.02	8.19	27,334	9.42	8.5	108,979	10.38	9.59	322,160
Sex of child (male = 1)	0.52	0.5	486,520	0.5	0.5	347,765	0.5	0.5	27,334	0.5	0.5	108,979	0.51	0.5	322,160
Birth order within household	2.11	1.61	486,520	2.8	2.36	347,765	2.86	2.54	27,334	2.86	2.36	108,979	3.1	2.48	322,160
Number of vaccinations	5.95	2.83	486,520	6.26	2.59	347,765	5.53	3.13	27,334	5.18	2.95	108,979	5.29	3.04	322,160
Age mother at birth (years)	23.1	5.49	486,520	24.14	6.86	347,765	23.98	7.05	27,334	24.05	6.97	108,979	24.87	7.02	322,160
Years of education (years)	6.5	4.96	486,520	6.13	4.01	347,765	5.23	3.61	27,334	6.19	4.19	108,979	3.87	4.32	322,160
Place of living (urban = 1)	0.3	0.46	486,520	0.26	0.44	347,765	0.35	0.48	27,334	0.41	0.49	108,979	0.32	0.47	322,160
Asset index deviation reg. mean	0.01	0.93	486,520	−0.04	0.78	347,765	−0.03	0.92	27,334	−0.02	0.8	108,979	−0.02	0.86	322,160
Number of people in household	6.83	3.08	486,520	6.28	2.88	347,765	6.24	2.87	27,334	7.5	3.74	108,979	7.94	4.36	322,160
Real per capita GDP	3200.47	1612.51	486,520	1556.15	1067.86	347,765	829.34	207.12	27,334	4309.1	3691.08	108,979	2244.1	1475.91	322,160
Drought index (scPDSI)	−0.76	0.98	486,520	−0.79	0.91	347,765	−0.38	0.8	27,334	−0.27	1.14	108,979	−0.69	0.64	322,160
Malaria incidence	0.016	0.012	486,520	0.004	0.003	347,765	0.016	0.004	27,334	0.003	0.001	108,979	0.003	0	322,160
Night-time light	6.47	11.92	486,520	2.59	9.53	347,765	0.21	1	27,334	2.7	8.74	108,979	2.52	8.77	322,160
Population density	761.95	1350.65	486,520	389.27	1358.41	347,765	82.33	106.01	27,334	523.82	1898.61	108,979	413.73	1717.75	322,160

Notes: Descriptive statistics using the height-for-age z-score as depended variable. Considering instead the weight-for-height z-score the results are altered only marginally. *Source:* DHS and various other sources described in Table A.1; calculations by authors.

Appendix C. Modelling approach

The observed anthropometric measures, stunting and wasting, approximate long-term and short-term nutritional deficiencies respectively. This is a common approach when modelling nutritional outcomes, since growth failures are characteristic for nutritional deficiencies (for literature approximating nutritional deficiencies using anthropometric measures, see among others, de Onis et al., 2000; Kandala et al., 2009, 2011; Osgood-Zimmerman et al., 2018). Using distributional structured additive regression, both parameters of the normal distribution, the mean μ, and the standard deviation σ of the response variables are related to the predictors $\boldsymbol{\eta_\mu}$ and $\boldsymbol{\eta_\sigma}$, respectively, which take the following form:

$$\begin{aligned} \boldsymbol{\eta}_{\mu} &= \boldsymbol{\eta}_{\mu}^{Socio-economic} + \boldsymbol{\eta}_{\mu}^{Georeferenced} + f_{13}(\texttt{Spatial}, \texttt{Time}) + \boldsymbol{x}'\boldsymbol{\gamma} \\ \boldsymbol{\eta}_{\sigma} &= \boldsymbol{\eta}_{\sigma}^{Socio-economic} + \boldsymbol{\eta}_{\sigma}^{Georeferenced} + f_{13}(\texttt{Spatial}, \texttt{Time}) + \boldsymbol{x}'\boldsymbol{\gamma}, \end{aligned} \tag{C.1}$$

where both predictors $\boldsymbol{\eta_\mu}$, and, $\boldsymbol{\eta_\sigma}$ contain the same set of covariates that will be specified further below, and subsume the two sub-predictors $\boldsymbol{\eta}^{Socio-economic}$ and $\boldsymbol{\eta}^{Georeferenced}$ (note that for reasons of readability the subscripts of the parameters are omitted). $f_{13}(\cdot)$ is a smooth spatio-temporal effect with Markov random field prior. Note that the neighbourhood structure for the spatio-temporal effect $f_{13}(\cdot)$ is defined such that it allows for a complex spatio-temporal interaction and resembles a tensor product approach. γ_1 and γ_2 are linear effects of the gender and the place of living, for which diffuse priors are assumed, such that $p(\gamma_i) \propto const$. In more detail, the two sub-predictors $\boldsymbol{\eta}^{Socio-economic}$ and $\boldsymbol{\eta}^{Georeferenced}$ contain socio-economic characteristics and georeferenced characteristics of the grid cells, respectively, as specified hereafter:

$$\begin{aligned} \boldsymbol{\eta}^{Socio-economic} = {} & f_1(\text{Asset index}) \\ & + f_2(\text{Birthorder, Age mother at birth}) \\ & + f_3(\text{Age child, Breastfeeding duration}) \\ & + f_4(\text{Education mother}) + f_5(\log(GDP)) \\ & + f_6(\text{Household size}) + f_7(\text{Survey year}) \\ & + f_8(\text{Number of vaccinations}), \end{aligned} \tag{C.2}$$

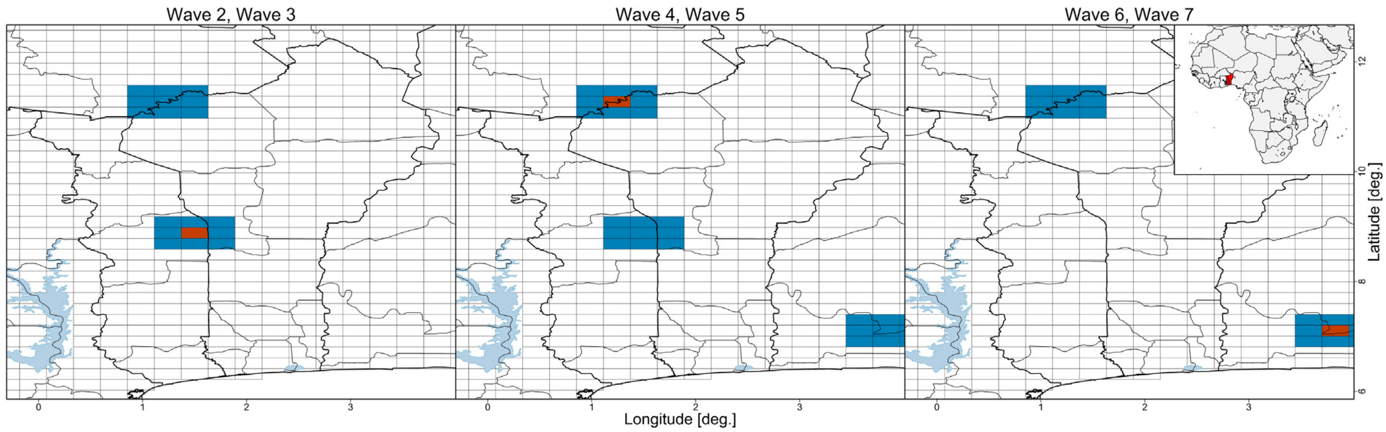

Fig. C.1. Illustration of the spatio-temporal interaction. *Notes:* Selected centre cells are shown in red, while their neighbours in space and time are shown in blue.

and,

$$\eta^{Georeferenced} = f_9(\text{Drought severity index}) + f_{10}(\text{Malaria endemicity}) + f_{11}(\log(1 + \text{Night} - \text{time light})) + f_{12}(\log(1 + \text{Population density})). \tag{C.3}$$

where in $\eta^{Socio-economic}$, $f_1(\cdot)$ to $f_8(\cdot)$ are assumed non-linear effects of socio-economic characteristics and in $\eta^{Georeferenced}$, $f_9(\cdot)$ to $f_{12}(\cdot)$ are assumed non-linear effects of georeferenced characteristics of the grid cells.[8] Note that due to the wide range of the values of some covariates (population density, the night-time light index and GDP), which are accompanied by large gaps, these covariates were log-transformed. The effects are modelled using Bayesian P-splines assuming as smoothness prior a second order random walk (Lang and Brezger, 2004). The spatio-temporal model is based on a fully Bayesian approach using Markov Chain Monte Carlo simulation for inference (Lang and Brezger, 2004; Brezger and Lang, 2006). See Table 1 for detailed information on the included covariates and their association with growth failures based on previous literature. In addition, consult Table B.2 for the summary statistics of the included covariates.

C.1 Spatio-temporal trends

Combining geostatistical approaches and additive models and aiming to map the response distribution while controlling for non-linear covariate effects at the same time is also known as geoadditive models (Kammann and Wand, 2003; Ruppert et al., 2003). A Markov random field prior is used to estimate the spatio-temporal development for which a complex interaction is assumed. Spatial information on the position of the primary sampling unit the household in which child i lives, is overlayed by a regular grid with a resolution of 25 × 25 km. The surface is projected using a cylindric equal area projection as the coordinate reference system. The indicator $l = 1, \ldots, L$ indexes the cells that form a connected geographical surface of the analysed region, which subsumes the neighbourhood structure of the cells to each other. Time is represented by the discrete index $t = 1, 2, 3$.[9] Assuming that spatial and temporal neighbouring cells resemble each other and are similar compared to non-neighbouring cells, allows for a spatio-temporal correlated smooth effect. Combining the available spatial information with the temporal information and building pairs l, t for each combination of l and t, allows to incorporate a spatially-temporally correlated smooth effect. See also Fig. C.1 for a schematic illustration, where red cells indicate centre cells and blue cells their neighbours across space and time.

A valid definition for the Markov random field prior can be achieved for each cell l, t by properly defining its neighbourhood structure across space and time. Two disjoint cells l, t and l', t' are assumed to be neighbours if they share a common border or follow successively in time. Thus the spatial smoothness prior for $f_{13}(\texttt{Spatial, Time})$ is given by $\beta_{l,t}|\beta_{l',t'}, l, t \neq l', t', \tau^2 \sim N(\frac{1}{N_{l,t}}\sum_{l',t' \in \delta_{l,t}} \beta_{l't'}, \frac{\tau^2}{N_{l,t}})$, where $N_{l,t}$ is the number of neighbouring cells across space and time, $l', t' \in \delta_{l,t}$ indicates that cell l', t' shares a common border across space and time with cell l, t (see also methodology manual of **BayesX**, Belitz et al., 2015, Chapter 4). Including a spatio-temporal effect $f_{13}(\texttt{Spatial, Time})$ accounts for heterogeneity across space and time not explained by the included socio-economic and remote sensed covariates.

C.2 Hierarchical model formulation

The geolocation of the sampling cluster a child resides in is located within a specific grid cell, which provides the spatial information that is used to incorporate a spatio-temporal effect. Remote sensed information is aggregated at the grid cell, as described previously. This gives rise to the reformulation of the model as a hierarchical or multilevel model, as observed children are nested into grid cells; this process is also referred to as clustering (Jain et al., 1999; Korenromp et al., 2004). Following Lang et al. (2014) the model described in Eq. (C.1) can be rewritten as

[8] Due to the high correlation ($\rho = 0.68$ for stunting) of the population density and the night-time light index, we included a two- dimensional effect in the model. This however, worsened the model fit significantly. Moreover, we estimated each model while omitting one of the two covariates. In the final model specifications only the population density is included, also due to the fact that for about 47% of the grid cells the value of the night-time light index is zero. After replacing values below 4, as suggested by Storeygard (2016), by the average value within an geographic unit, still around 7% of the grid cell are zero. This is also reflected when comparing the final model with the model including the adjusted index, using the DIC and the WAIC, which in almost all regions favours the first model.

[9] To guarantee that most countries are represented at all time points, instead of the year of the survey, respectively, the wave of the survey, the corresponding waves are aggregated as follows: Wave 2, Wave 3; Wave 4, Wave 5; Wave 6, Wave 7.

Table C.1
Model selection: Differences DIC and WAIC to Model 5.

Variable	Model	South Asia		Eastern SSA		MDG		Central SSA		Western SSA	
		Δ DIC	Δ WAIC	Δ DIC	Δ WAIC	Δ DIC	Δ WAIC	Δ DIC	Δ WAIC	Δ DIC	Δ WAIC
Stunting	Model 1	49,410	47,890	39,180	37,450	5199	4932	15,884	14,946	46,960	45,460
	Model 2	490	560	140	140	−1	−7	21	18	120	150
	Model 3	−20	−20	10	0	−4	−5	5	−3	30	20
	Model 4	93,620	93,390	72,540	72,340	7881	7711	25,913	25,626	58,100	57,860
	Model 5	0	0	0	0	0	0	0	0	0	0
	Model 6	−1980	−1930	−6800	−6530	**-907**	**-817**	**−5509**	**−4976**	**−7510**	**−7170**
	Model 7	**−1990**	**−1940**	**−6810**	**−6540**	−892	−808	−5496	−4965	−7490	−7160
Wasting	Model 1	42,170	41,010	34,470	33,170	3515	3298	14,330	13,382	46,300	44,990
	Model 2	630	670	310	310	9	12	57	57	260	280
	Model 3	30	20	40	40	10	8	12	7	40	40
	Model 4	26,800	26,870	23,070	23,280	3663	3577	10,750	10,588	20,520	20,550
	Model 5	0	0	0	0	0	0	0	0	0	0
	Model 6	−1990	−1950	**−6530**	**−6280**	−408	**-375**	**−4925**	**−4472**	−6930	−6550
	Model 7	**−2010**	**−1970**	**−6530**	−6260	**-409**	−374	**−4925**	−4469	**−6940**	**−6560**

Notes: Lowest information criteria are in bold. Results are shown for Model 7. *Source:* DHS; calculation by authors.

multilevel model as follows:

$$\begin{aligned}\textbf{Level}-\mathbf{1}: \quad \eta_\mu \quad &= \quad \eta_\mu^{Socio-}\boldsymbol{economic} + \boldsymbol{x}'\boldsymbol{\gamma}\\ &+ f_{13}(Spatial, Time)\textbf{Level}-\mathbf{2}{:}f_{13}(Spatial, Time)\\ &= \eta_\mu^{Georeferenced} + f_{13,5}(Spatial, Time)\textbf{Level}-\mathbf{1}{:}\eta_\sigma\\ &= \eta_\sigma^{Socio-}\boldsymbol{economic} + \boldsymbol{x}'\boldsymbol{\gamma}\\ &+ f_{13}(Spatial, Time)\textbf{Level}-\mathbf{2}{:}f_{13}(\text{Spatial}, \text{Time})\\ &= \eta_\sigma^{Georeferenced} + f_{13,5}(\text{Spatial}, \text{Time}). \end{aligned} \tag{C.4}$$

Reformulating Eq. (C.1) and accounting for the hierarchical data structure described above,[10] yields Eq. (C.4), where the distributional structured additive predictor is rewritten as a predictor representing the hierarchical structure. Development over space and time for the mean μ and the standard deviation σ are captured by the level-2 equations of $f_{13}(\texttt{Spatial}, \texttt{Time})$, which include besides the spatio-temporal effect $f_{13}(\cdot)$ the remote sensed data aggregated at the grid cell subsumed in $\eta_\mu^{Georeferenced}$ and $\eta_\sigma^{Georeferenced}$, respectively.

C.3 Model selection

The goodness-of-fit of each model is first evaluated using the deviance information criterion (DIC) (Spiegelhalter et al., 2002) and the widely applicable information criterion (WAIC) (Watanabe, 2010). Both information criteria can be seen as generalisation of the Akaike information criterion (AIC), and the lower the values of the DIC and the WAIC, the better the model fits the data. Second, insignificant covariates and interactions are gradually removed by inspecting the significance of the included covariate and interaction using simultaneous Bayesian credible intervals (Krivobokova et al., 2010).

The final model is constructed using the following procedure. Starting with Eq. (C.4) and omitting the predictor η_σ, the model complexity is gradually increased, distinguishing between different model specifications according to the following scheme:

- Model 1: Multilevel additive model (MAM) equation (C.4), including available potential determinants of childhood undernutrition, omitting the predictor η_σ.
- Model 2: MAM equation (C.4), including $\eta_\mu^{Socio-economic}$, $\eta_\sigma^{Socio-economic}$, $\eta_\mu^{Georeferenced}$, $\eta_\sigma^{Georeferenced}$, omitting the spatio-temporal effect $f_{13,5}(\texttt{Spatial}, \texttt{Time})$ in both predictors η_μ and η_σ.
- Model 3: MAM equation (C.4), omitting $\eta_\mu^{Georeferenced}$ and $\eta_\sigma^{Georeferenced}$.
- Model 4: Eq. (C.4), omitting $\eta_\mu^{Socio-economic}$ and $\eta_\sigma^{Socio-economic}$.
- Model 5: MAM equation (C.4).
- Model 6: Eq. (C.4), explicitly accounting for disparities between boys and girls.
- Model 7: MAM equation (C.4), removing insignificant effects in η_μ and η_σ.

Table C.1 summarises the information criteria for each model, where we see the following effects. First, by not accounting for heterogeneity and omitting the predictor η_σ for the standard deviation, the model fit is drastically worse in all regions. Similarly, solely relying on remote sensed determinants and omitting individual and household specific socio-economic determinants does not cover all aspects of malnutrition and yields a poorer fit compared to the model specified in Eq. (C.4), and thus results in a poor model fit. Second, omitting the spatial effect also results in a poorer model fit. Third, by using a gender-specific varying coefficient (Hastie and Tibshirani, 1993) for the spatial effect (and thus accounting for gender differences directly), the model improves relative to the model specified in Eq. (C.4). Together, these effects emphasise that the socio- economic determinants of malnutrition play a crucial role, and it is not sufficient to rely purely on remote sensed data as in, for example Osgood-Zimmerman et al. (2018).

[10] Moreover, computational speed and mixing of the parameters sampled via MCMC simulation techniques improves.

Appendix D. Randomised quantile residuals

D.1 Stunting

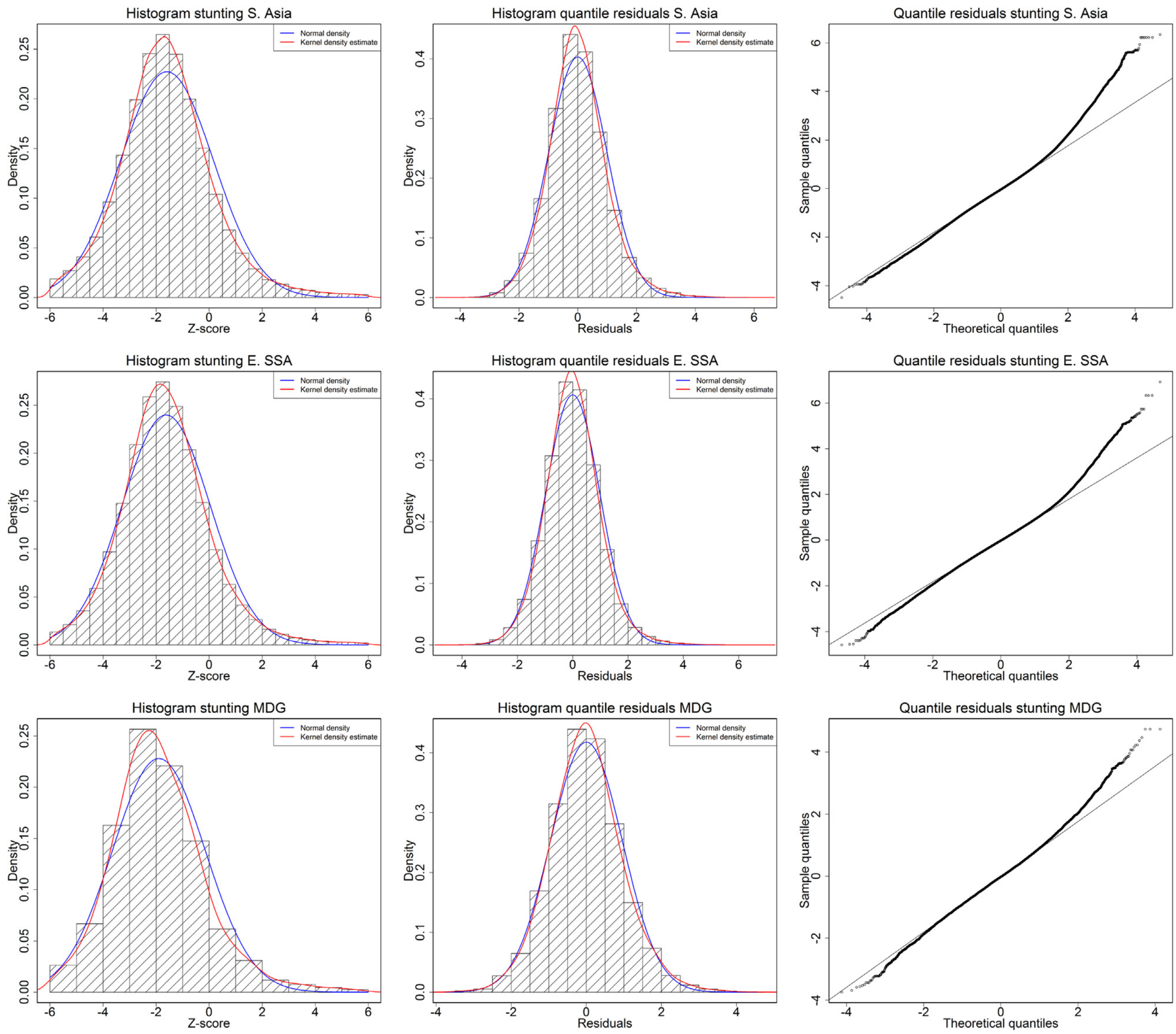

Fig. D.1. Randomised quantile residuals of the height-for-age z-score. *Notes:* The left hand panels show the histograms of the height-for-age z-score together with a kernel density estimate and a Gaussian density. The middle panels show the histograms of the randomised quantile residuals together with a kernel density estimate and a Gaussian density. The right hand panels show the randomised quantile residuals against their theoretical quantiles. The first row depicts the estimates for South Asia, the second row the estimates for Eastern sub-Saharan Africa, and the third row the estimates for Madagascar.

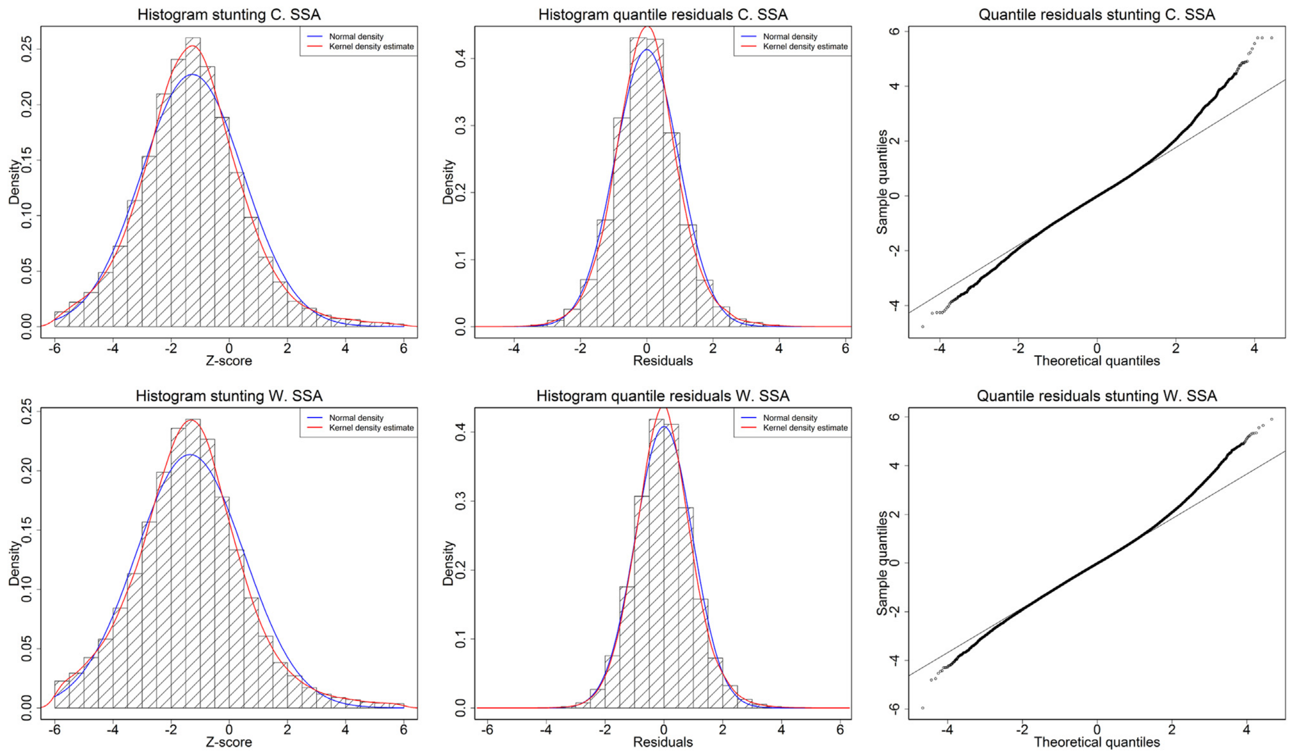

Fig. D.2. Randomised quantile residuals of the height-for-age z-score. *Notes:* The left hand panels show the histograms of the height-for-age z-score together with a kernel density estimate and a Gaussian density. The middle panels show the histograms of the randomised quantile residuals together with a kernel density estimate and a Gaussian density. The right hand panels show the randomised quantile residuals against their theoretical quantiles. The first row shows the estimates for Central sub-Saharan Africa, while in the second row the estimates for Western sub-Saharan Africa are shown.

D.2 Wasting

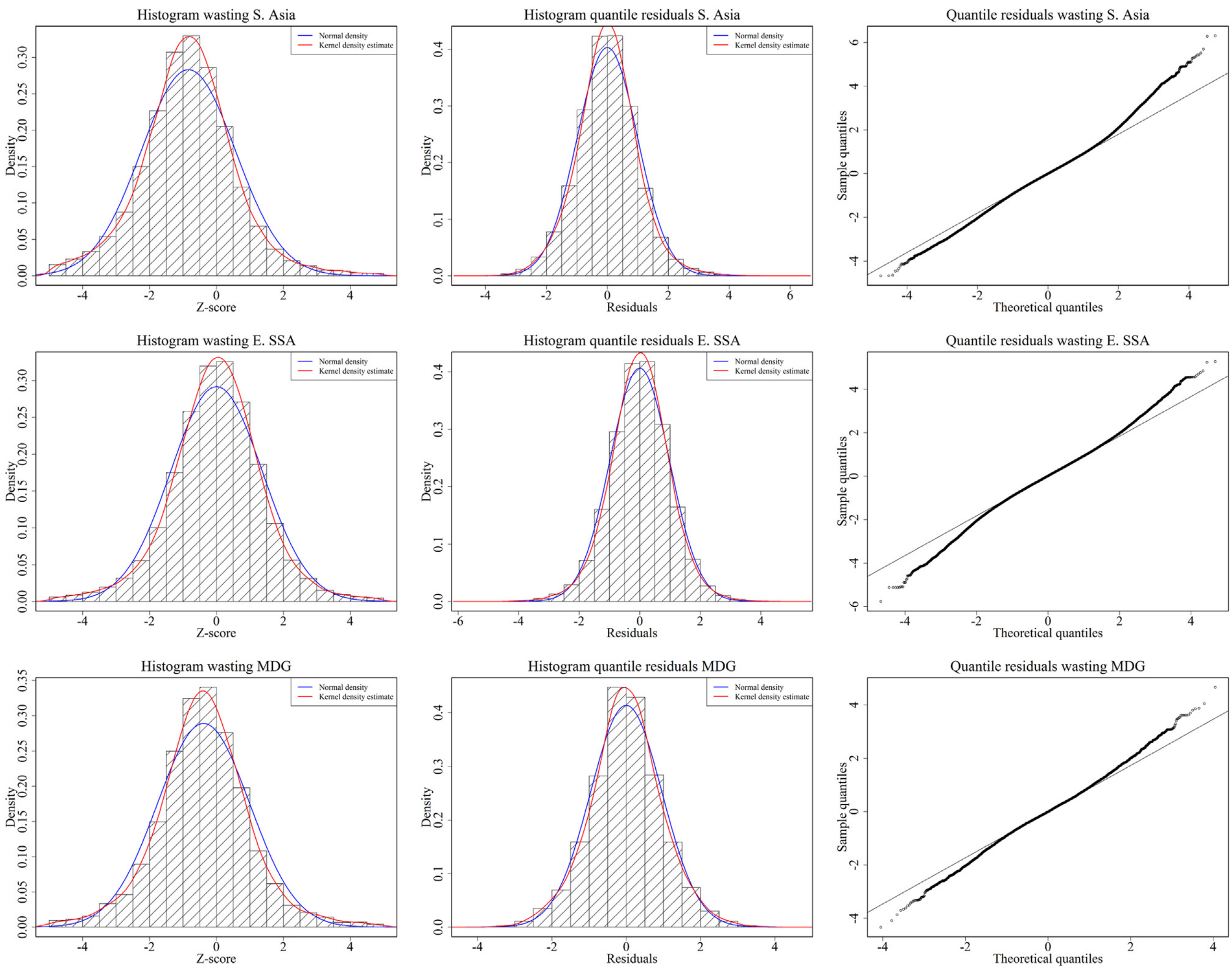

Fig. D.3. Randomised quantile residuals of the weight-for-height z-score. *Notes:* The left hand panels show the histograms of the weight-for-height z- score together with a kernel density estimate and a Gaussian density. The middle panels show the histograms of the randomised quantile residuals together with a kernel density estimate and a Gaussian density. The right hand panels show the randomised quantile residuals against their theoretical quantiles. The first row depicts the estimates for South Asia, the second row the estimates for Eastern sub-Saharan Africa, and the third row the estimates for Madagascar.

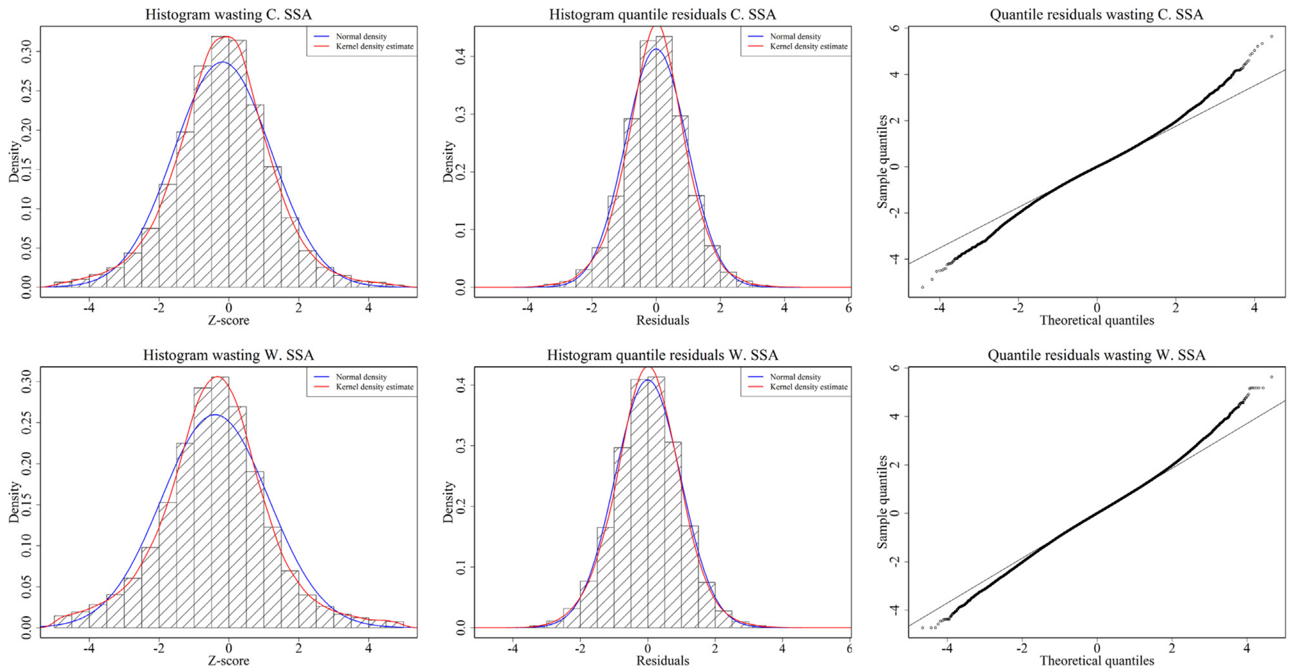

Fig. D.4. Randomised quantile residuals of the weight-for-height z-score. *Notes:* The left hand panels show the histograms of the weight-for-height-score together with a kernel density estimate and a Gaussian density. The middle panels show the histograms of the randomised quantile residuals together with a kernel density estimate and a Gaussian density. The right hand panels show the randomised quantile residuals against their theoretical quantiles. The first row shows the estimates for Central sub-Saharan Africa, while in the second row the estimates for Western sub-Saharan Africa are shown.

Appendix E. Marginal effects wasting

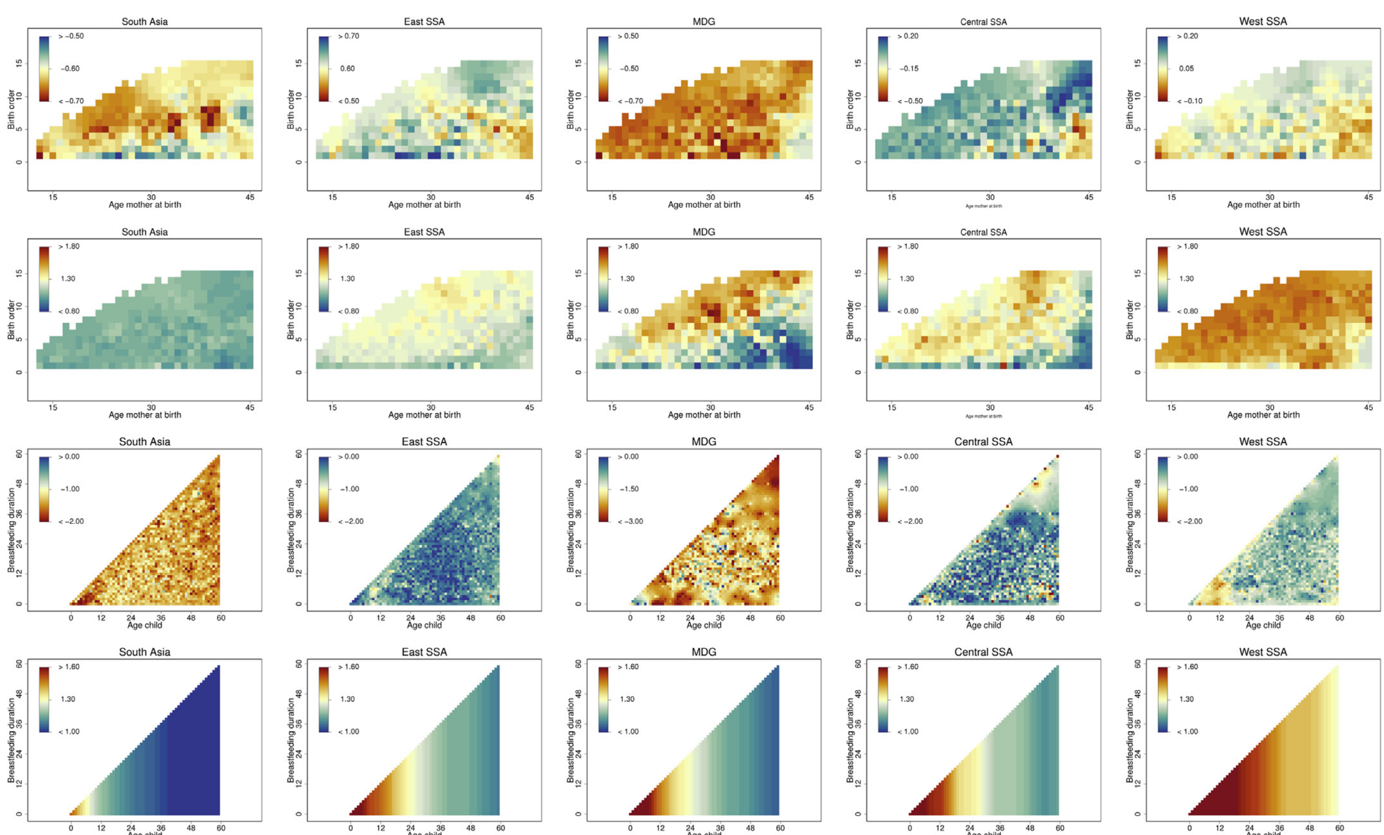

Fig. E.1. Marginal effects on the weight-for-height z-score for the interaction of the age of the mother and the birth order of the child (top), and the interaction of the age of the child and breastfeeding duration (bottom) for South Asia, Eastern sub-Saharan Africa, Madagascar, Central sub-Saharan Africa, and Western sub- Saharan Africa. *Notes:* The even lines of the panel show the marginal effects on the mean μ, while the odd lines of the panel show the marginal effect on the standard deviation σ. Note that the colour range differs due illustration purposes. *Source:* DHS; calculations by the authors.

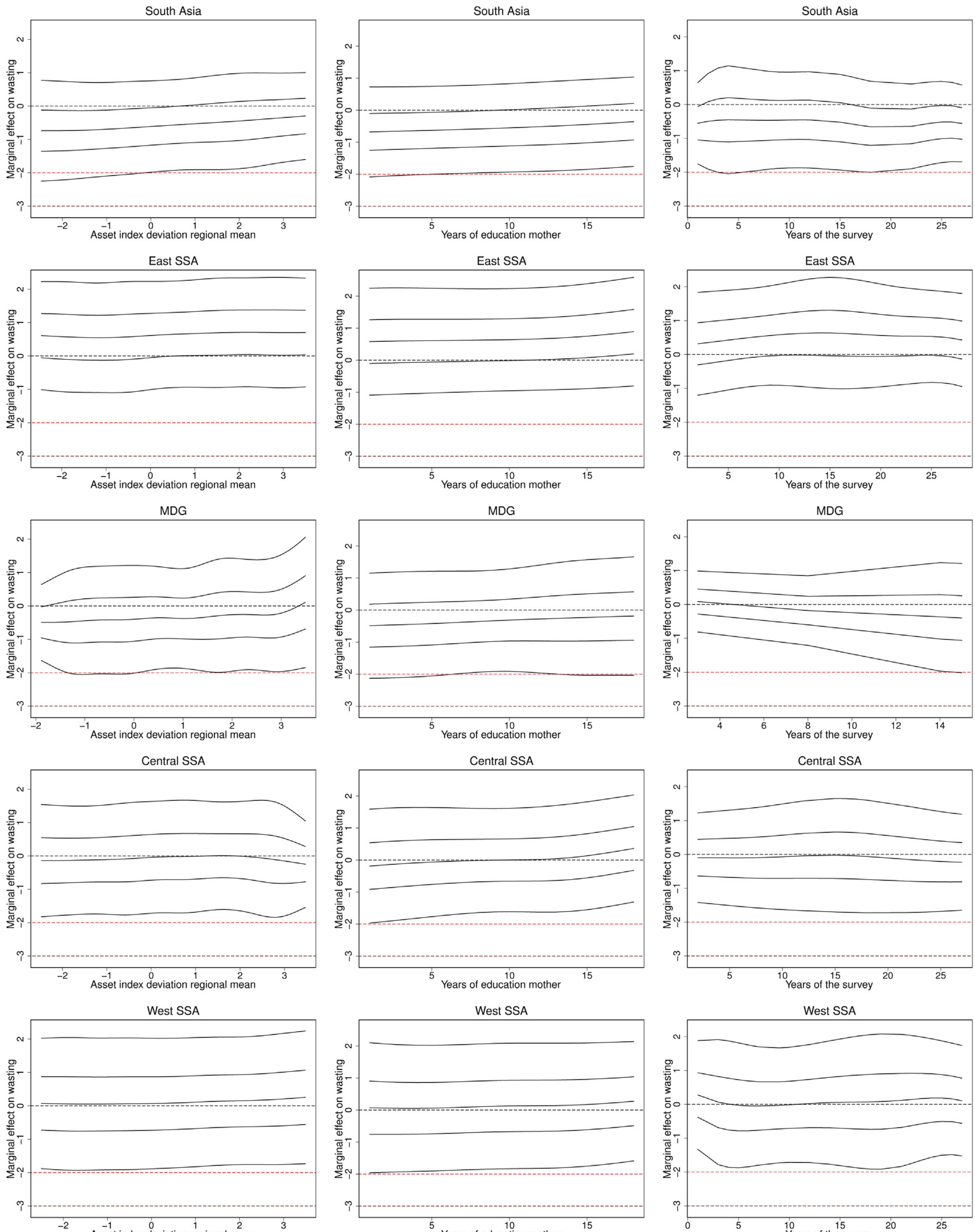

Fig. E.2. Marginal effects on the weight-for-height z-score of the asset index (first column), the years of education of the mother (second column), and the year of the survey (third column), together with the 10%, 30%, 70% and 90% quantiles for South Asia, Eastern sub-Saharan Africa, Madagascar, Central sub-Saharan Africa, and Western sub-Saharan Africa. *Source:* DHS; calculations by the authors.

References

Aizawa, T., 2019. Ex-ante inequality of opportunity in child malnutrition: new evidence from ten developing countries in Asia. Econ. Hum. Biol. 35, 144–161. doi:http://dx.doi.org/10.1016/j.ehb.2019.06.003.

Akombi, B.J., Agho, K.E., Merom, D., Renzaho, A.M., Hall, J.J., 2017. Child malnutrition in sub-Saharan Africa: a meta-analysis of demographic and health surveys (2006–2016). PLOS ONE 12, 1–11. doi:http://dx.doi.org/10.1371/journal.pone.0177338.

Alderman, H., Lokshin, M., Radyakin, S., 2011. Tall claims: mortality selection and the height of children in India. Econ. Hum. Biol. 9, 393–406. doi:http://dx.doi.org/10.1016/j.ehb.2011.04.007.

Amoah, B., Giorgi, E., Heyes, D.J., van Burren, S., Diggle, P.J., 2018. Geostatistical modelling of the association between malaria and child growth in Africa. Int. J. Health Geogr. 17, 7. doi:http://dx.doi.org/10.1186/s12942-018-0127-y.

Arnold, F., 1997. Gender Preferences for Children. DHS Comparative Studies No. 23. Macro International Inc., Calverton, Maryland, USA. http://dhsprogram.com/pubs/pdf/CS23/CS23.pdf.

Ayele, D.G., Zewotir, T.T., Mwambi, H.G., 2015. Structured additive regression models with spatial correlation to estimate under-five mortality risk factors in Ethiopia. BMC Public Health 15, 268. doi:http://dx.doi.org/10.1186/s12889-015-1602-z.

Barichivich, J., Osborn, T.J., Harris, I., van der Schrier, G., Jones, P.D., 2018. Drought. State of the Climate in 2018, vol. 100. (under review).

Bauer, J.M., Mburu, S., 2017. Effects of drought on child health in Marsabit District, Northern Kenya. Econ. Hum. Biol. 24, 74–79. doi:http://dx.doi.org/10.1016/j.ehb.2016.10.010.

Belitz, C., Brezger, A., Klein, N., Kneib, T., Lang, S., Umlauf, N., 2015. BayesX: Software for Bayesian Inference in Structured Additive Regression Models. Version 3.0.2. . http://www.BayesX.org/.

Belitz, C., Hübner, J., Klasen, S., Lang, S., 2010. Determinants of the Socioeconomic and Spatial Pattern of Undernutrition by Sex in India: A Geoadditive Semi-parametric Regression Approach. Physica-Verlag HD, Heidelberg, pp. 155–179. doi:http://dx.doi.org/10.1007/978-3-7908-2413-1_9.

Black, R.E., Allen, L.H., Bhutta, Z.A., Caulfield, L.E., de Onis, M., Ezzati, M., Mathers, C., Rivera, J., 2008. Maternal and child undernutrition: global and regional exposures and health consequences. Lancet 371, 243–260. doi:http://dx.doi.org/10.1016/S0140-6736(07)61690-0.

Black, R.E., Victora, C.G., Walker, S.P., Bhutta, Z.A., Christian, P., de Onis, M., Ezzati, M., Grantham-McGregor, S., Katz, J., Martorell, R., Uauy, R., 2013. Maternal and child undernutrition and overweight in low-income and middle-income countries. Lancet 382, 427–451. doi:http://dx.doi.org/10.1016/S0140-6736(13)60937-X.

Breierova, L., Duflo, E., 2004. The Impact of Education on Fertility and Child Mortality: Do Fathers Really Matter Less Than Mothers? Working Paper 10513. National Bureau of Economic Research doi:http://dx.doi.org/10.3386/w10513.

Brezger, A., Lang, S., 2006. Generalized structured additive regression based on Bayesian P-splines. Comput. Stat. Data Anal. 50, 967–991. doi:http://dx.doi.org/10.1016/j.csda.2004.10.011.

Brown, M.E., Grace, K., Shively, G., Johnson, K.B., Carroll, M., 2014. Using satellite remote sensing and household survey data to assess human health and nutrition response to environmental change. Popul. Environ. 36, 48–72. doi:http://dx.doi.org/10.1007/s11111-013-0201-0.

Bryce, J., Boschi-Pinto, C., Shibuya, K., Black, R.E., 2005. WHO estimates of the causes of death in children. Lancet 365, 1147–1152. doi:http://dx.doi.org/10.1016/S0140-6736(05)71877-8.

Center for International Earth Science Information Network – CIESIN – Columbia University, 2017. Gridded Population of the World, Version 4 (GPWv4): Population Density, Revision 10. doi:http://dx.doi.org/10.7927/H49C6VHW.

Center for International Earth Science Information Network – CIESIN – Columbia University, and Centro Internacional de Agricultura Tropical - CIAT, 2005. Gridded Population of the World, Version 3 (GPWv3): Population Density Grid. doi:http://dx.doi.org/10.7927/H4XK8CG2.

Dancer, D., Rammohan, A., Smith, M.D., 2008. Infant mortality and child nutrition in Bangladesh. Health Econ. 17, 1015–1035. doi:http://dx.doi.org/10.1002/hec.1379.

de Onis, M., Blössner, M., Borghi, E., 2012. Prevalence and trends of stunting among pre-school children, 1990–2020. Public Health Nutr. 15, 142–148. doi:http://dx.doi.org/10.1017/S1368980011001315.

de Onis, M., Frongillo, E.A., Blössner, M., 2000. Is malnutrition declining? An analysis of changes in levels of child malnutrition since 1980. Bull. World Health Organ. 78, 1222–1233.

Dunn, P.K., Smyth, G.K., 1996. Randomized quantile residuals. J. Comput. Graph. Stat. 5, 236–244. doi:http://dx.doi.org/10.1080/10618600.1996.10474708.

Feenstra, R.C., Inklaar, R., Timmer, M.P., 2015. The next generation of the Penn World Table. Am. Econ. Rev. 105, 3150–3182. doi:http://dx.doi.org/10.1257/aer.20130954.

Fenske, N., Burns, J., Hothorn, T., Rehfuess, E.A., 2013. Understanding child stunting in India: a comprehensive analysis of socio-economic, nutritional and environmental determinants using additive quantile regression. PLOS ONE 8, 1–16. doi:http://dx.doi.org/10.1371/journal.pone.0078692.

Filmer, D., Pritchett, L.H., 2001. Estimating wealth effects without expenditure data – or tears: an application to educational enrollments in states of India. Demography 38, 115–132. doi:http://dx.doi.org/10.1353/dem.2001.0003.

Frongillo, Edward A.J., de Onis, M., Hanson, K.M., 1997. Socioeconomic and demographic factors are associated with worldwide patterns of stunting and wasting of children. J. Nutr. 127, 2302–2309. doi:http://dx.doi.org/10.1093/jn/127.12.2302.

Gayawan, E., Adebayo, S.B., Komolafe, A.A., Akomolafe, A.A., 2019. Spatial distribution of malnutrition among children under five in Nigeria: a Bayesian quantile regression approach. Appl. Spat. Anal. Policy 12, 229–254. doi:http://dx.doi.org/10.1007/s12061-017-9240-8.

Gething, P.W., Elyazar, I.R.F., Moyes, C.L., Smith, D.L., Battle, K.E., Guerra, C.A., Patil, A. P., Tatem, A.J., Howes, R.E., Myers, M.F., George, D.B., Horby, P., Wertheim, H.F.L., Price, R.N., Müeller, I., Baird, J.K., Hay, S.I., 2012. A long neglected world malaria map: Plasmodium vivax endemicity in 2010. PLOS Negl. Trop. Dis. 6, 1–12. doi:http://dx.doi.org/10.1371/journal.pntd.0001814.

Grace, K., Davenport, F., Funk, C., Lerner, A.M., 2012. Child malnutrition and climate in sub-Saharan Africa: an analysis of recent trends in Kenya. Appl. Geogr. 35, 405–413. doi:http://dx.doi.org/10.1016/j.apgeog.2012.06.017.

Grépin, K.A., Bharadwaj, P., 2015. Maternal education and child mortality in Zimbabwe. J. Health Econ. 44, 97–117. doi:http://dx.doi.org/10.1016/j.jhealeco.2015.08.003.

Haile, D., Azage, M., Mola, T., Rainey, R., 2016. Exploring spatial variations and factors associated with childhood stunting in Ethiopia: spatial and multilevel analysis. BMC Pediatr. 16, 49. doi:http://dx.doi.org/10.1186/s12887-016-0587-9.

Harttgen, K., Lang, S., Seiler, J., 2019. Selective mortality and the anthropometric status of children in low- and middle-income countries. Econ. Hum. Biol. 34, 257–273. doi:http://dx.doi.org/10.1016/j.ehb.2019.04.001.

Hastie, T.J., Tibshirani, R.J., 1993. Varying-coefficient models. J. R. Stat. Soc. Ser. B (Methodological) 55, 757–796. http://www.jstor.org/stable/2345993.

Hathi, P., Haque, S., Pant, L., Coffey, D., Spears, D., 2017. Place and child health: the interaction of population density and sanitation in developing countries. Demography 54, 337–360. doi:http://dx.doi.org/10.1007/s13524-016-0538-y.

Hatton, T.J., Sparrow, R., Suryadarma, D., van der Eng, P., 2018. Fertility and the health of children in Indonesia. Econ. Hum. Biol. 28, 67–78. doi:http://dx.doi.org/10.1016/j.ehb.2017.12.002.

Jain, A.K., Murty, M.N., Flynn, P.J., 1999. Data clustering: a review. ACM Comput. Surv. 31, 264–323. doi:http://dx.doi.org/10.1145/331499.331504.

Johnson, K., Brown, M.E., 2014. Environmental risk factors and child nutritional status and survival in a context of climate variability and change. Appl. Geogr. 54, 209–221. doi:http://dx.doi.org/10.1016/j.apgeog.2014.08.007.

Kammann, E.E., Wand, M.P., 2003. Geoadditive models. J. R. Stat. Soc. Ser. C (Appl. Stat.) 52, 1–18. doi:http://dx.doi.org/10.1111/1467-9876.00385.

Kandala, N.B., Fahrmeir, L., Klasen, S., Priebe, J., 2009. Geo-additive models of childhood undernutrition in three sub-Saharan African countries. Popul. Space Place 15, 461–473. doi:http://dx.doi.org/10.1002/psp.524.

Kandala, N.B., Madungu, T.P., Emina, J.B., Nzita, K.P., Cappuccio, F.P., 2011. Malnutrition among children under the age of five in the Democratic Republic of Congo (DRC): does geographic location matter? BMC Public Health 11, 261. doi:http://dx.doi.org/10.1186/1471-2458-11-261.

Kandala, N.B., Mandungu, T.P., Mbela, K., Nzita, K.P., Kalambayi, B.B., Kayembe, K.P., Emina, J.B.O., 2014. Child mortality in the Democratic Republic of Congo: cross-sectional evidence of the effect of geographic location and prolonged conflict from a national household survey. BMC Public Health 14, 266. doi:http://dx.doi.org/10.1186/1471-2458-14-266.

Klein, N., Kneib, T., Klasen, S., Lang, S., 2015a. Bayesian structured additive distributional regression for multivariate responses. J. R. Stat. Soc. Ser. C (Appl. Stat.) 64, 569–591. doi:http://dx.doi.org/10.1111/rssc.12090.

Klein, N., Kneib, T., Lang, S., Sohn, A., 2015b. Bayesian structured additive distributional regression with an application to regional income inequality in Germany. Ann. Appl. Stat. 9, 1024–1052. doi:http://dx.doi.org/10.1214/15-AOAS823.

Korenromp, E., Arnold, F., Williams, B., Nahlen, B., Snow, R., 2004. Monitoring trends in under-5 mortality rates through national birth history surveys. Int. J. Epidemiol. 33, 1293–1301. doi:http://dx.doi.org/10.1093/ije/dyh182.

Krivobokova, T., Kneib, T., Claeskens, G., 2010. Simultaneous confidence bands for penalized spline estimators. J. Am. Stat. Assoc. 105, 852–863. doi:http://dx.doi.org/10.1198/jasa.2010.tm09165.

Lai, Y.S., Biedermann, P., Ekpo, U.F., Garba, A., Mathieu, E., Midzi, N., Mwinzi, P., N'Goran, E.K., Raso, G., Assaré, R.K., Sacko, M., Schur, N., Talla, I., Tchuenté, L.A.T., Touré, S., Winkler, M.S., Utzinger, J., Vounatsou, P., 2015. Spatial distribution of schistosomiasis and treatment needs in sub-Saharan Africa: a systematic review and geostatistical analysis. Lancet Infect. Dis. 15, 927–940. doi:http://dx.doi.org/10.1016/S1473-3099(15)00066-3.

Lang, S., Brezger, A., 2004. Bayesian P-splines. J. Comput. Graph. Stat. 13, 183–212. http://www.jstor.org/stable/1391151.

Lang, S., Umlauf, N., Wechselberger, P., Harttgen, K., Kneib, T., 2014. Multilevel structured additive regression. Stat. Comput. 24, 223–238. doi:http://dx.doi.org/10.1007/s11222-012-9366-0.

Li, X., Zhou, Y., Zhao, M., Zhao, X., 2020. A harmonized global nighttime light dataset 1992–2018. Sci. Data 7, 168. doi:http://dx.doi.org/10.1038/s41597-020-0510-y.

López-Carr, D., Mwenda, K.M., Pricope, N.G., Kyriakidis, P.C., Jankowska, M.M., Weeks, J., Funk, C., Husak, G., Michaelsen, J., 2016. Climate-related child undernutrition in the Lake Victoria basin: an integrated spatial analysis of health surveys, NDVI, and precipitation data. IEEE J. Sel. Top. Appl. Earth Obs. Remote Sens. 9, 2830–2835. doi:http://dx.doi.org/10.1109/JSTARS.2016.2569411.

Makate, M., Makate, C., 2016. The causal effect of increased primary schooling on child mortality in Malawi: universal primary education as a natural experiment. Soc. Sci. Med. 168, 72–83. doi:http://dx.doi.org/10.1016/j.socscimed.2016.09.003.

National Geophysical Data Center, n.d. Image and Data Processing by NOAA's National Geophysical Data Center. DMSP Data Collected by US Air Force Weather Agency. https://ngdc.noaa.gov/eog/dmsp/downloadV4composites.html. (Accessed 7 September 2018).
Osgood-Zimmerman, A., Millear, A.I., Stubbs, R.W., Shields, C., Pickering, B.V., Earl, L., Graetz, N., Kinyoki, D.K., Ray, S.E., Bhatt, S., Browne, A.J., Burstein, R., Cameron, E., Casey, D.C., Deshpande, A., Fullman, N., Gething, P.W., Gibson, H.S., Henry, N.J., Herrero, M., Krause, L.K., Letourneau, I.D., Levine, A.J., Liu, P.Y., Longbottom, J., Mayala, B.K., Mosser, J.F., Noor, A.M., Pigott, D.M., Piwoz, E.G., Rao, P., Rawat, R., Reiner, R.C., Smith, D.L., Weiss, D.J., Wiens, K.E., Mokdad, A.H., Lim, S.S., Murray, C.J.L., Kassebaum, N.J., Hay, S.I., 2018. Mapping child growth failure in Africa between 2000 and 2015. Nature 555, 41–47. doi:http://dx.doi.org/10.1038/nature25760.
Pelletier, D.L., Frongillo, E.A., 2003. Changes in child survival are strongly associated with changes in malnutrition in developing countries. J. Nutr. 133, 107–119.
Pelletier, D.L., Frongillo, E.A., Schroeder, D.G., Habicht, J.P., 1995. The effects of malnutrition on child mortality in developing countries. Bull. World Health Organ. 73, 443–448. http://www.ncbi.nlm.nih.gov/pmc/articles/PMC2486780/.
R Core Team, 2016. R: A Language and Environment for Statistical Computing. R Foundation for Statistical Computing, Vienna, Austria. https://www.R-project.org/.
Rakotomanana, H., Gates, G.E., Hildebrand, D., Stoecker, B.J., 2017. Determinants of stunting in children under 5 years in Madagascar. Matern. Child Nutr. 13, e12409. doi:http://dx.doi.org/10.1111/mcn.12409.
Ruppert, D., Wand, M.P., Carroll, R.J., 2003. Semiparametric Regression. Cambridge Series in Statistical and Probabilistic Mathematics. Cambridge University Press doi:http://dx.doi.org/10.1017/CBO9780511755453.
Sahn, D.E., Stifel, D., 2003. Exploring alternative measures of welfare in the absence of expenditure data. Rev. Income Wealth 49, 463–489. doi:http://dx.doi.org/10.1111/j. 0034-6586.2003.00100.x.
Savory, D.J., Andrade-Pacheco, R., Gething, P.W., Midekisa, A., Bennett, A., Sturrock, H.J.W., 2017. Intercalibration and Gaussian process modeling of nighttime lights imagery for measuring urbanization trends in Africa 2000–2013. Remote Sens. 9. doi:http://dx.doi.org/10.3390/rs9070713.
Schmidt-Traub, G., De la Mothe Karoubi, E., Espey, J., 2015. Indicators and a Monitoring Framework for the Sustainable Development Goals: Launching a Data Revolution for the SDGs. Technical ReportUnited Nations Sustainable Development Solutions Network. . . (Accessed 24 September 2019) http://unsdsn.org/wp-content/uploads/2015/03/150320-SDSN-Indicator-Report.pdf.
van der Schrier, G., Barichivich, J., Briffa, K.R., Jones, P.D., 2013. A scPDSI-based global data set of dry and wet spells for 1901–2009. J. Geophys. Res: Atmos. 118, 4025–4048. doi:http://dx.doi.org/10.1002/jgrd.50355.
Smith, L.C., Haddad, L., 2015. Reducing child undernutrition: past drivers and priorities for the post-MDG era. World Dev. 68, 180–204. doi:http://dx.doi.org/10.1016/j.worlddev.2014.11.014.
Spears, D., 2013. How Much International Variation in Child Height Can Sanitation Explain? Policy Research Working Paper No. WPS 6351. World Bank, Washington, DC, USA. http://documents.worldbank.org/curated/en/449651468191643600/How-much-international-variation-in-child-height-can-sanitation-explain.
Spiegelhalter, D.J., Best, N.G., Carlin, B.P., Van der Linde, A., 2002. Bayesian measures of model complexity and fit. J. R. Stat. Soc. Ser. B (Stat. Methodol.) 64, 583–639. http://www.jstor.org/stable/3088806.
Storeygard, A., 2016. Farther on down the road: transport costs, trade and urban growth in sub-Saharan Africa. Rev. Econ. Stud. 83, 1263–1295. doi:http://dx.doi.org/10.1093/restud/rdw020.
Umlauf, N., Adler, D., Kneib, T., Lang, S., Zeileis, A., 2015. Structured additive regression models: an R interface to BayesX. J. Stat. Softw. 63, 1–46. doi:http://dx.doi.org/10.18637/jss.v063.i21.
Umlauf, N., Klein, N., Zeileis, A., 2018a. BAMLSS: Bayesian additive models for location, scale, and shape (and beyond). J. Comput. Graph. Stat. 27, 612–627. doi:http://dx.doi.org/10.1080/10618600.2017.1407325.
Umlauf, N., Kneib, T., Klein, N., 2018b. BayesX: R Utilities Accompanying the Software Package BayesX. R Package Version 0.3-0. . https://CRAN.R-project.org/package=BayesX.
United Nations, 2015. United Nations Decade of Action on Nutrition. Technical ReportUnited Nations, New York, USA. . . (Accessed 14 March 2019). http://www.un.org/ga/search/view_doc.asp?symbol=A/70/L.42.
United Nations Children's Fund, 1990. Strategy for Improved Nutrition of Children and Women in Developing Countries. A UNICEF Policy Review. United Nations Children's Fund, New York, USA.
United Nations Children's Fund, 2013. Improving Child Nutrition: The Achievable Imperative for Global Progress. United Nations Children's Fund, New York, USA.
United Nations Children's Fund, World Health Organization, International Bank for Reconstruction and Development/The World Bank, 2017. Levels and Trends in Child Malnutrition: Key Findings of the 2017 Edition of the Joint Child Malnutrition Estimates. World Health Organization, Geneva, Switzerland.
United Nations Children's Fund, World Health Organization, International Bank for Reconstruction and Development/The World Bank, 2019. Levels and Trends in Child Malnutrition: Key Findings of the 2019 Edition of the Joint Child Malnutrition Estimates. World Health Organization, Geneva, Switzerland.
Vollmer, S., Harttgen, K., Kupka, R., Subramanian, S.V., 2017. Levels and trends of childhood undernutrition by wealth and education according to a Composite Index of Anthropometric Failure: evidence from 146 Demographic and Health Surveys from 39 countries. BMJ Glob. Health 2, e000206. doi:http://dx.doi.org/10.1136/bmjgh-2016-000206.
Watanabe, S., 2010. Asymptotic equivalence of Bayes cross validation and widely applicable information criterion in singular learning theory. J. Mach. Learn. Res. 11, 3571–3594.
World Health Organization, 1999. Management of Severe Malnutrition: A Manual for Physicians and Other Senior Health Workers. World Health Organization, Geneva, Switzerland.
World Health Organization, 2013. Guide: Updates on the Management of Severe Acute Malnutrition in Infants and Children. World Health Organization, Geneva, Switzerland.
World Health Organization, 2017. The Double Burden of Malnutrition. Policy Brief. Word Health Organization, Geneva, Switzerland.
World Health Organization Multicentre Growth Reference Study Group, 2006. WHO Child Growth Standards: Length/Height-for-Age, Weight-for-Age, Weight-for-Length, Weight-for-Height and Body Mass Index-for-Age: Methods and Development. World Health Organization, Geneva, Switzerland.
World Health Organization Multicentre Growth Reference Study Group, de Onis, M., 2006. Assessment of differences in linear growth among populations in the WHO Multicentre Growth Reference Study. Acta Paediatr. 95, 56–65.
Zeileis, A., Hornik, K., Murrell, P., 2009. Escaping RGBland: selecting colors for statistical graphics. Comput. Stat. Data Anal. 53, 3259–3270. doi:http://dx.doi.org/10.1016/j.csda.2008.11.033.